Spring 2021

Supercritical and Subcritical Pitchfork Bifurcations in a Buckling Problem for a Graphene Sheet Between two Rigid Substrates

Jake Grdadolnik
jmg317@zips.uakron.edu

SUPERCRITICAL AND SUBCRITICAL PITCHFORK BIFURCATIONS IN A BUCKLING PROBLEM FOR A GRAPHENE SHEET BETWEEN 2 RIGID SUBSTRATES

A Thesis

Presented to

The Graduate Faculty of The University of Akron

In Partial Fulfillment

of the Requirements for the Degree

Master of Science

Jake Matthew Grdadolnik

May, 2021

SUPERCRITICAL AND SUBCRITICAL PITCHFORK BIFURCATIONS IN A BUCKLING PROBLEM FOR A GRAPHENE SHEET BETWEEN 2 RIGID SUBSTRATES

Jake Matthew Grdadolnik

Department of Mathematics

Honors Research Project

Submitted to

The Williams Honors College
The University of Akron

Approved:

Date: 4/15/21
Honors Project Sponsor (signed)

J. Pat Wilber
Honors Project Sponsor (printed)

Date: 06/14/21
Reader (signed)

Dmitry Golovaty
Reader (printed)

Date: 04/14/21
Reader (signed)

Alexander Hoover
Reader (printed)

Accepted:

Date: 4/15/21
Honors Department Advisor (signed)

Curtis B. Clemons
Honors Department Advisor (printed)

Kevin Kreider Date: 4/15/21
Department Chair (signed)

Dr Kevin Kreider, Mathematics
Department Chair (printed)

ABSTRACT

In this paper we study a model of the buckling of a sheet of graphene between two rigid substrates. We seek to understand the buckling of the sheet as the substrate separation is varied with a fixed load on each end of the sheet. We write down the expression for total energy of the system and from it derive a 2-point nonlinear boundary-value problem whose solutions are equilibrium configurations of the sheet. We cannot get an explicit solution. Instead, we perform a bifurcation analysis by using asymptotics to approximate solutions on the bifurcating branches near the bifurcation points. The bifurcating parameter is the separation between the rigid substrates. We find that the bifurcations are supercritical or subcritical pitchfork bifurcations. We perform a parametric study to understand how the nature of the bifurcations is influenced by other physical parameters in the problem. This leads to insight on the orientation of the buckled graphene sheet depending on substrate separation.

TABLE OF CONTENTS

LIST OF TABLES

LIST OF FIGURES

CHAPTER I

INTRODUCTION

1.1 Graphene

We begin with an introduction to the material we will be working with, graphene, and with a description of a buckling problem for graphene that motivates the study. Graphene is a single-layer of graphite, and is grouped into the family of carbon-based nanomaterials [3]. Graphene is made up of a one atom thick layer of sp^2 hybridized carbon atoms, making it a 2D material [4]. The atoms in this layer are arranged in a hexagonal lattice. See Figure 1.1. Any other material that is one atom think is also described as a 2D material. These sp^2 bonds are extremely strong and account for several of the basic mechanical properties of graphene [4]. In particular, these bonds make it difficult to change the distance between neighboring atoms in the lattice and to change the angles formed by two neighboring bonds. Also, the bonds try to keep nearby atoms in the same plane. As a consequence, graphene is very strong in tension and has a resistance to bending. In addition, the larger surface area of graphene along with some other useful properties to be discussed makes it more useful than some of its relatives [3].

Graphene is often synthesized in bilayers or suspended over a rigid substrate

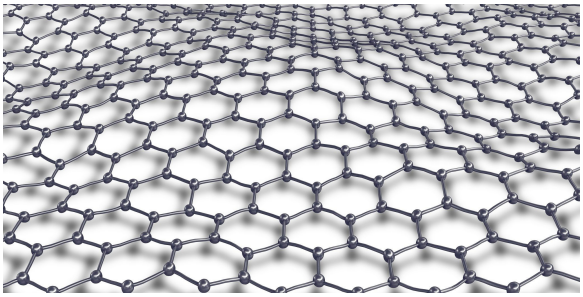

Figure 1.1: Image of the 2D material Graphene from [1]

material. The two layers in bilayer graphene interact with each other by Van der Waals forces between the atoms on different layers. Likewise graphene interacts with a rigid substrate by Van der Waals forces between the atoms on the layer and the atoms on the substrate. These complicated interatomic forces can be modeled crudely with the Lennard-Jones Potential [5].

This potential typically contains a paramater σ called the Van der Waals radius. When the two atoms are closer than σ, the force is repulsive. When they are σ apart, the force acting upon them is 0. When they are further than σ, the force is attractive. As the atoms get further apart however, the force becomes closer and closer in magnitude to 0. As they get closer, the repulsive force blows up to infinity. These Van der Waals forces are present in all molecules and are very weak. When two graphene sheets interact, the energy associated with the Van der Waals forces is minimized when the sheets are approximately σ apart, similar to the scenario described with the carbon atoms.

Graphene has been the subject of extensive study in part because of its

excellent material properties. In this paragraph we discuss the mechanical properties of graphene. In terms of 2D materials, strength refers to the maximum stress a 2D material can maintain [6]. Graphene, with a strength of 130 GPa, is stronger than all other competitors such as Phosphorene and Silicene [6]. In addition, the elastic properties of graphene result in a higher Young's Modulus than the competitors as well with graphene at 345 N/m where h-BN and MoS_2 have values of 271 N/m and 141 N/m respectively [6]. We also note that graphene can be viewed as the fundamental building block for other carbon nanostructures like carbon nanotubes [6]. Hence these other nanostructures inherit many of their mechanical properties from the mechanical properties of graphene.

Due to graphene having excellent electronic mobility and high mechanical resilience, the material has possible applications in transparent flexible electronics, such as foldable displays and transparent solar cells [7]. However, the mechanical deformation of graphene has an effect on these electronic properties [7]. Similarly, graphene has important optical properties making it useful for application in medical optics and photonics [7]. Again we note that when graphene is deformed, its optical properties, such as the optical conductivity or transparency, may change [7].

Graphene also has excellent thermal properties. For example, graphene has an unusually high in-plane thermal conductivity [8]. In terms of thermal application, due to graphene having such a high thermal conductivity, this could relate to lower temperature rise when used in nanoscale devices [8]. This would result in devices, for instance cell phones, growing less hot in the phone user's hands because graphene

could be used as a heat sink [8]. Again we note these properties change when deformation occurs. The underlying theme is that these important properties of graphene are dependent on the state of deformation of graphene. One must understand mechanics in the deformation of graphene even if one is mainly interested in an application involving electronic, optical, or thermal properties.

1.2 Problem Motivation

A layered solid is defined as a solid whose deformation is constrained to two-dimensions [9, 10]. Explaining the confined deformation of layered solids when subject to edge loads is an active area of research in materials science [9, 10, 2, 11]. It is well established that when the basal planes of layered solids are loaded edge-on, they generally fail by the formation of kink bands. See Figure 1a in [9]. A recently proposed micromechanism responsible for the formation of kink bands and more generally important for the deformation of layered solids is ripplocations. Kushima et al. introduced the term ripplocation to describe deformations that occur in layered materials [11]. A ripplocation is a localized ripple or fold in a single layer of a layered material.

To provide macroscopic evidence for ripplocations, in [2] Barsoum et al. reported the results of a buckling experiment in which various layered materials were placed between two constraining fixed blocks. One block is fixed and the other block can translate in the transverse direction, i.e. perpendicular to the direction of the undeformed layers. See Figure 1.2. The edges were loaded to study the buckling

and ripplocations in the layered materials [2]. We note that an idealized model was created to study the buckling by Barsoum et al. but in the following paper we study a more sophisticated model.

1.3 Problem Description and Analysis

In [2], the authors report experimental results for several different layered materials. In particular, results for the constant edge-loading of graphite are reported. Graphite has the structure of stacked or layered graphene sheets. See Figure 1.2 (e). We use the experiment from Barsoum et al. to motivate the modeling and analysis of the buckling of a single layer of graphene sandwiched between 2 rigid substrates. This simplified model can serve as a first step to understanding the multilayered graphene experiments of Barsoum et al.

For the model, we have two rigid parallel substrates above and below a single deformable graphene layer. Note that this model is rotated from the experimental set up depicted in Figure 1.2. We then apply a fixed load β to each end of the deformable layer and vary the distance D between the rigid substrates. We assume that the graphene layer interacts with each of the substrates by Van der Waals forces. When D is relatively small, so that both the upper and the lower substrates strongly repel the layer, the substrates provide a transverse load that is compressive in the sense that it tries to keep the the layer unbuckled. Loosely speaking, the layer is squeezed between the substrates. The layer also has an intrinsic resistance to bending that tries to keep it unbuckled. On the other hand, the load β on the edges tries to make

the layer buckle. If we start with D small and increase the value of D, while keeping β fixed, there should be a critical D at which the layer buckles.

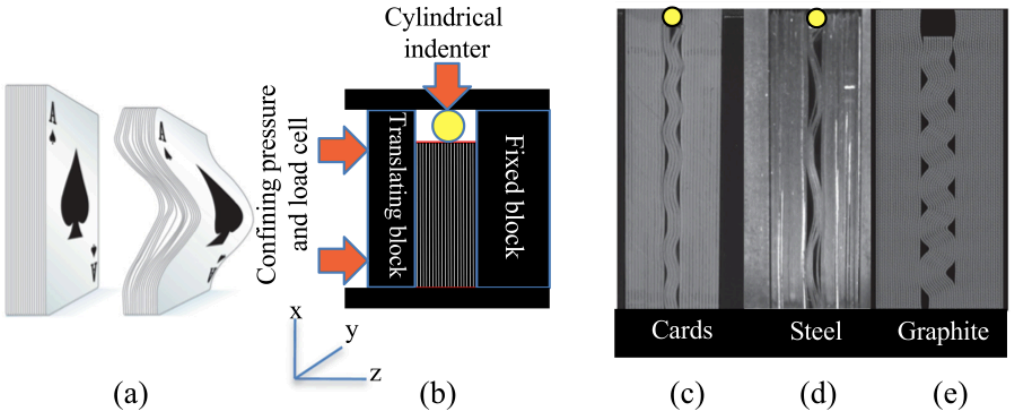

Figure 1.2: Experimental setup from Barsoum et al. investigating buckling in multilayered materials from [2].

We will derive the total energy of this system in an attempt to model the buckling of the graphene layer. After deriving the total energy of the system, we compute the Euler-Lagrange equation for the total energy. This results in a system of 4 first-order differential equations from which we form a 2-point nonlinear boundary-value problem for equilibrium solutions to the problem. We cannot solve this boundary-

value problem analytically.

After rescaling, there are 4 parameters in the problem. These are ω, the Van der Waals strength, σ, the Van der Waals radius, β, the edge load, and D, the separation between the substrates. The goal is to construct a bifurcation diagram for the problem, where D is the bifurcation parameter. To do this, we must first find the points where the geometry of the system changes qualitatively, these are known as bifurcation points. We determine a trivial branch for the bifurcation diagram. We interpret the trivial branch physically as the deformable graphene layer in its unbuckled configuration, in which the layer is flat, parallel to the substrates, and in a position midway between the substrates. To locate bifurcation points, we linearize the problem about a typical solution on the trivial branch. To analyze the linearized 2-point bvp, we are able to convert the system of first-order equations into a single fourth-order linear differential equation. For a given ω and σ, we can find a curve in the βD-plane that gives, for a given positive β, the smallest value of D at which the layer buckles out of the trivial configuration. Using numerical techniques, we determine this curve of first bifurcations points for different values of ω and σ.

We then approximate the curves that describe the nontrivial branches that bifurcate off the trivial branch at the bifurcation points. In order to approximate these bifurcating branches locally near the bifurcation points, we return to the linear 2-point bvp and employ asymptotic techniques. Specifically, we assume regular expansions for the solutions on the bifurcation branches and a regular expansion for the bifurcation parameter D. In the usual way, this yields a sequence of linear

problems for the coefficients in the expansions. Using the $\mathcal{O}(\epsilon^2)$ system, $\mathcal{O}(\epsilon^3)$ system, and solvability conditions from the Fredholm Alternative Theorem, we are able to determine coefficients in the expansion for the bifurcation parameter D. We discover that $D_1 = 0$ for typical values of ω and σ. We then investigate the sign of D_2, which determines if we have a supercritical or subcritical pitchfork bifurcation at the bifurcation point.

1.4 Subcritical and Supercritical Pitchfork Bifurcations

To justify the significance of the sign of D_2, in this section we present some elementary background on pitchfork bifurcations. We are now going to investigate two scalar-valued first-order differential equations and create their bifurcation diagrams in order to explain the implications of a supercritical versus subcritical pitchfork bifurcation. Consider first the equation

$$x' = x(r - x^2). \tag{1.1}$$

To sketch the bifucation diagram, we first need to identify fixed points. We see that if

$$x(r - x^2) = 0, \tag{1.2}$$

then either

$$x = 0, x = \pm\sqrt{r}, \tag{1.3}$$

where the later pair of solutions exist only for $r > 0$. This results in the following bifurcation diagram shown in Figure 1.3.

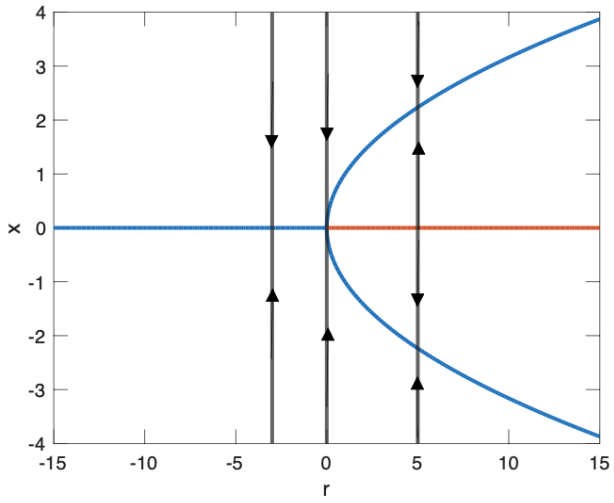

Figure 1.3: Bifurcation diagram showing supercritical pitchfork bifurcation at the bifurcation point $r = 0$ for (1.1). The blue branches are stable, and the orange branches are unstable. The black lines are typical phaselines.

In Figure 1.3 we see the resulting supercritical pitchfork bifurcation. The key feature of this diagram is that the branch that emanates from the trivial branch is stable, so that at the bifurcation point the trivial solution bifurcates to a solution that is 'close to' the trivial solution. If (1.1) modeled the deformation of a beam, for example, then the model would predict only an initial slight bending of the beam, which may have important structural implications.

Now we will consider the second equation

$$x' = x(r + x^2 - x^4). \tag{1.4}$$

We again need to identify fixed points, which are found by solving

$$x(r + x^2 - x^4) = 0. \tag{1.5}$$

We see that fixed points for (1.4) are

$$x = 0, x = \pm\sqrt{\frac{1 \pm \sqrt{1-4r}}{2}}. \tag{1.6}$$

This results in the bifucation diagram depicted in Figure 1.4.

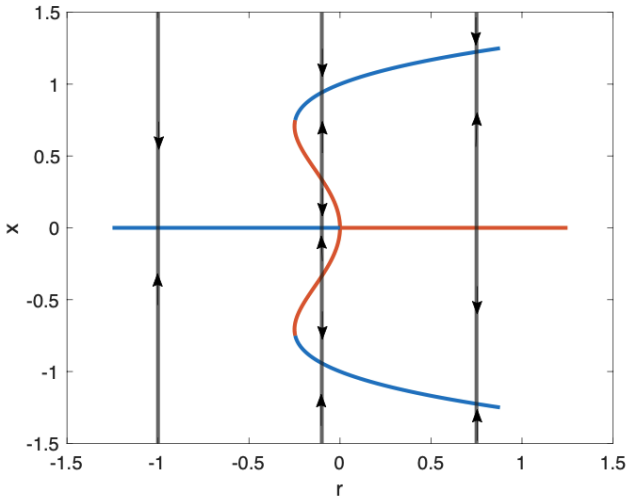

Figure 1.4: Bifurcation diagram showing subcritical pitchfork bifurcation at the bifurcation point $r = 0$ for (1.4). The blue branches are stable, and the orange branches are unstable. The black lines are typical phaselines.

In Figure 1.4 we see the resulting subcritical pitchfork bifurcation. The main difference between the bifurcations for (1.1) and (1.4) is that the branches for the supercritical pitchfork that emanate from the trivial branch are unstable. At the bifurcation point, the trivial solution bifurcates, through some dynamical process, to a solution that is 'far from' trivial solution. Returning to the beam analogy, the model (1.4) could predict that the beams shape deforms dramatically, which could be associated with structural failure.

1.5 Main Results

We conclude this introduction by summarizing the main results of this thesis. Before we can discuss this however, we need to talk about how these results relate to supercritical and subcritical bifurcations. By a combination of asymptotics and numerical computations, we find the first 2 terms in the expansion for the bifurcation parameter D. We show that D_1 is typically zero and we investigate the sign of D_2, the second coefficient in this expansion. The significance is that whether the bifurcation is subcritical or supercritical is determined by the sign of D_2. We assume that the trivial branch is stable for values of D less than the first bifurcation point and that the trivial branch loses stability at the first bifurcation point. From this it follows that if $D_2 > 0$ we see a supercritical bifurcation, and if $D_2 < 0$ we see a subcritical bifurcation. As discussed in the previous subsection, this second case may correspond to a drastic change in the state of deformation of the layer as we increase through this bifurcation point because the solution may jump to a buckled configuration far from the trivial configuration.

For the problem, after creating plots to determine the sign of D_2 for various combinations of parameters, we find that there is some interval of β where D_2 is negative. This interval of β is unique for different σ and ω. When σ is fixed and ω is varied, increasing the value of ω causes this interval where the D_2 curve is negative to grow wider, with the left endpoint moving towards zero and the right endpoint increasing to larger values of β. Similarly, when σ is varied and ω is fixed, we see

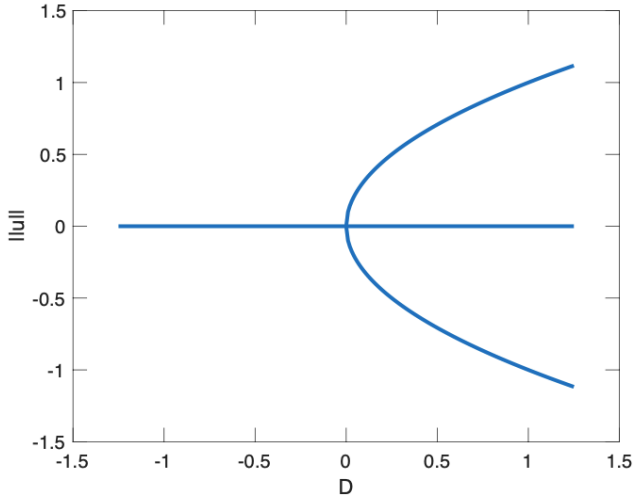

Figure 1.5: Supercritical bifurcation when $D_2 > 0$ where $||u||$ measures the size of the solution to the problem.

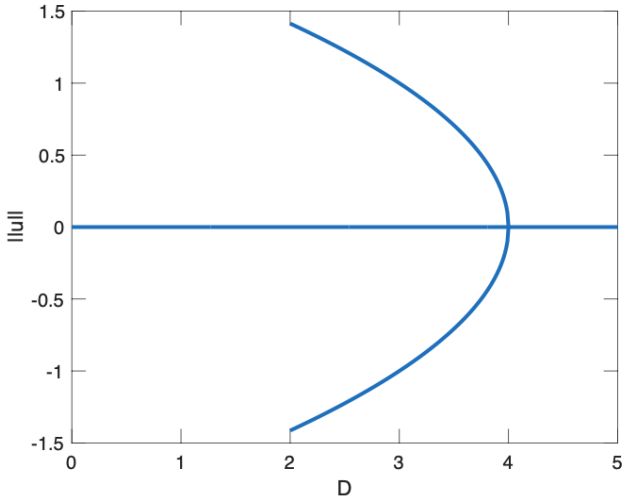

Figure 1.6: Subcritical bifurcation when $D_2 < 0$ where $||u||$ measures the size of the solution to the problem.

the same behavior of the D_2 curves. Additionally, if the values of σ and ω are too small or too large, then we have no change in sign and D_2 is either fully positive or fully negative over the viewing interval. We can infer then that when we have a combination of parameters that contains a sign change, increasing the edge-load β causes large changes in the buckling of the system.

CHAPTER II

ENERGY EQUATION

We begin to study a graphene layer between two rigid parallel substrates a distance D apart. Additionally, we assume the deformable graphene layer interacts with the substrates by Van der Waals forces. To study the buckling, we apply compressive edge loads of magnitude β parallel to the substrates. We also assume the layer deforms the same in every cross-section, so we can study just the deformation of a typical cross-section.

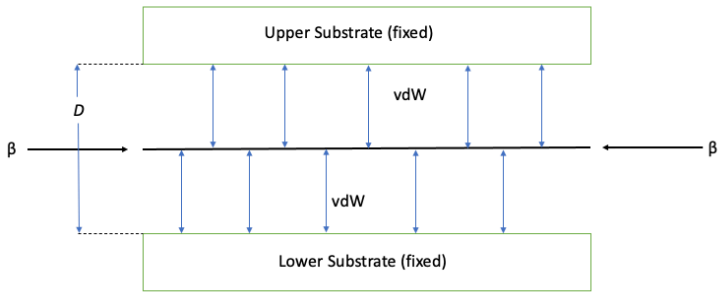

Figure 2.1: Cross-section of the buckling problem.

We will refer to the cross-section seen in Figure 2.1 as a rod. We parameterize

the rod with

$$\hat{r}(s) = x(s)\hat{i} + y(s)\hat{j} \quad 0 \leq s \leq L, \tag{2.1}$$

where L is the length of the rod.

Now we write down the total energy for the problem. We note that there are three pieces to the total energy. These are the bending energy of the rod, the Van der Waals interaction energy between the rod and the upper and lower substrates, and the work from the applied edge load.

Let us first derive the bending energy of the rod. We assume that the rod is inextensible. Consider the following diagram.

Figure 2.2: Deformation of inextensible rod.

Assuming the rod is inextensible means that the length of any section of the rod in the reference configuration cannot change under deformation. See Figure 2.2. So if we assume that the rod is inextensible and use the arc length formula we have

$$s - a = \int_a^s |\hat{r}'(\sigma)| d\sigma. \tag{2.2}$$

Taking the derivative with respect to s and using the Fundamental Theorem of Calculus we have

$$|\hat{r}'(s)| = 1. \tag{2.3}$$

Differentiating (2.1) with respect to s we have

$$\hat{r}'(s) = x'(s)\hat{i} + y'(s)\hat{j}. \tag{2.4}$$

On the other hand, since $\hat{r}'$ is a unit vector, there is an angle θ such that

$$\hat{r}'(s) = cos(\theta(s))\hat{i} + sin(\theta(s))\hat{j}. \tag{2.5}$$

We reach the equations

$$x'(s) = cos(\theta(s)), \tag{2.6}$$

$$y'(s) = sin(\theta(s)). \tag{2.7}$$

Note that θ is the angle that the tangent vector to the rod makes with the positive x-axis. Using the definition of curvature from calculus we see that

$$\frac{|\hat{T}'(s)|}{|\hat{r}'(s)|} = \frac{|\theta'(s)|}{1} = |\theta'(s)|, \tag{2.8}$$

where $\hat{T}$ is the unit tangent vector for the rod. We define the bending energy by

$$\frac{\kappa}{2} \int_0^L [\theta'(s)]^2 ds, \tag{2.9}$$

where $\kappa > 0$ is a constant called the bending modulus.

Now for the Van der Waals interaction energy. We assume that the Van der Waals interaction between a point on the rod and the upper or lower substrate depends only on the vertical distance between the point and the substrate. Therefore we model this energy with

$$\int_0^L V(y(s))ds + \int_0^L V(D - y(s))ds, \tag{2.10}$$

where V is given by the Lennard Jones potential 9-3

$$V(y) = \omega \left(\left(\frac{\sigma}{y} \right)^9 - \left(\frac{\sigma}{y} \right)^3 \right), \tag{2.11}$$

with ω and σ defining the strength and radius of the Van der Waals respectively. Additionally, we introduce

$$\int_0^L \gamma_1(s)[y'(s) - \sin(\theta(s))]ds + \int_0^L \gamma_2(s)[x'(s) - \cos(\theta(s))]ds, \tag{2.12}$$

where γ_1 and γ_2 are Lagrange multipliers. These terms enforce the inextensibility constraint. Finally, we subtract off the work of the applied edge load

$$\beta x(0) - \beta x(L). \tag{2.13}$$

Thus the total energy equation becomes

$$\begin{aligned} E[x, y, \theta] = \frac{\kappa}{2} \int_0^L [\theta'(s)]^2 ds + \int_0^L V(y(s))ds + \int_0^L V(D - y(s))ds \\ + \int_0^L \gamma_1(s)[y'(s) - \sin(\theta(s))]ds + \int_0^L \gamma_2(s)[x'(s) - \cos(\theta(s))]ds \\ - \beta x(0) + \beta x(L). \end{aligned} \tag{2.14}$$

Next we derive the governing equations by computing the Euler-Lagrange equations of the total energy (2.14). Let $(\bar{x}, \bar{y}, \bar{\theta})$ be a minimizer of E. First we take

$$\frac{\partial}{\partial \epsilon} E[x, y, \bar{\theta} + \epsilon\theta]\Big|_{\epsilon=0} \tag{2.15}$$

$$\begin{aligned} =&\frac{\partial}{\partial \epsilon}\left[\frac{\kappa}{2}\int_0^L [\bar{\theta}' + \epsilon\theta']^2 ds + \int_0^L \gamma_1(s)[y'(s) - \sin(\bar{\theta} + \epsilon\theta)]ds\right]_{\epsilon=0} \qquad (2.16)\\ &+ \frac{\partial}{\partial \epsilon}\left[\int_0^L \gamma_2(s)[x'(s) - \cos(\bar{\theta} + \epsilon\theta)]ds\right]_{\epsilon=0} \end{aligned}$$

$$= \int_0^L \kappa(\bar{\theta}' + \epsilon\theta')\theta' ds - \int_0^L \gamma_1 \cos(\bar{\theta} + \epsilon\theta)\theta ds + \int_0^L \gamma_2 \sin(\bar{\theta} + \epsilon\theta)\theta ds\Big|_{\epsilon=0} \tag{2.17}$$

$$= \int_0^L \kappa(\bar{\theta}')\theta' ds - \int_0^L \gamma_1 \cos(\bar{\theta})\theta ds + \int_0^L \gamma_2 \sin(\bar{\theta})\theta ds \tag{2.18}$$

$$= -\int_0^L \kappa(\bar{\theta}'')\theta ds + \kappa\bar{\theta}'\theta\Big|_0^L - \int_0^L \gamma_1 \cos(\bar{\theta})\theta ds + \int_0^L \gamma_2 \sin(\bar{\theta})\theta ds \tag{2.19}$$

$$= -\int_0^L (\kappa\bar{\theta}'' + \gamma_1 \cos(\bar{\theta}) - \gamma_2 \sin(\bar{\theta}))\theta ds + \kappa\bar{\theta}'\theta\Big|_0^L . \tag{2.20}$$

So we reach the first equation

$$\kappa\bar{\theta}'' + \gamma_1 \cos(\bar{\theta}) - \gamma_2 \sin(\bar{\theta}) = 0 \ , \bar{\theta}'(0) = \bar{\theta}'(L) = 0. \tag{2.21}$$

Next we take

$$\frac{\partial}{\partial \epsilon} E[x, \bar{y} + \epsilon y, \theta]\Big|_{\epsilon=0} \tag{2.22}$$

$$\begin{aligned} &= \frac{\partial}{\partial \epsilon}\left[\int_0^L V(\bar{y} + \epsilon y)ds + \int_0^L V(D - (\bar{y} + \epsilon y))\right] ds \qquad (2.23)\\ &\quad + \frac{\partial}{\partial \epsilon}\left[\int_0^L \gamma_1[\bar{y}' + \epsilon y' - \sin(\theta(s))]ds\right]_{\epsilon=0} \end{aligned}$$

$$= \int_0^L V'(\bar{y}) y ds - \int_0^L V'(D - \bar{y}) y ds + \int_0^L \gamma_1 y' ds \tag{2.24}$$

$$= \int_0^L V'(\bar{y})yds - \int_0^L V'(D-\bar{y})yds - \int_0^L \gamma_1' yds + \gamma_1 y|_0^L \tag{2.25}$$

$$= \int_0^L (V'(\bar{y}) - V'(D-\bar{y}) - \gamma_1')yds + \gamma_1 y|_0^L \,. \tag{2.26}$$

So we reach the second equation

$$V'(\bar{y}) - V'(D-\bar{y}) - \gamma_1' = 0 \,, \gamma_1(0) = \gamma_1(L) = 0. \tag{2.27}$$

For the last equation we compute

$$\frac{\partial}{\partial \epsilon} E[\bar{x} + \epsilon x, y, \theta]\Big|_{\epsilon=0} \tag{2.28}$$

$$= \frac{\partial}{\partial \epsilon}\left[\int_0^L \gamma_2[\bar{x}' + \epsilon x' - \cos(\theta)]ds - \beta(\bar{x}(0) + \epsilon x(0)) + \beta(\bar{x}(L) + \epsilon x(L))\right]_{\epsilon=0} \tag{2.29}$$

$$= \int_0^L \gamma_2 x' ds - \beta x(0) + \beta x(L)\Big|_{\epsilon=0} \tag{2.30}$$

$$= \int_0^L \gamma_2 x' ds - \beta x(0) + \beta x(L) \tag{2.31}$$

$$= -\int_0^L \gamma_2' x ds + \gamma_2 x|_0^L - \beta x(0) + \beta x(L) \tag{2.32}$$

$$= -\int_0^L \gamma_2' x ds + \gamma_2(L)x(L) - \gamma_2(0)x(0) - \beta x(0) + \beta x(L) \tag{2.33}$$

$$= -\int_0^L \gamma_2' x ds + (\gamma_2(L) + \beta)x(L) - (\gamma_2(0) + \beta)x(0). \tag{2.34}$$

From which we reach

$$\gamma_2'(s) = 0 \,, \gamma_2(L) = -\beta \,, \gamma_2(0) = -\beta. \tag{2.35}$$

So we see that $\gamma_2 = -\beta$.

Since we know now $\gamma_2 = -\beta$ we can replace γ_2 in the previous equations and relabel γ_1 as γ. Relabeling θ' as ν we have the 2-point bvp

$$\gamma' = V'(y) - V'(D - y), \tag{2.36}$$

$$\kappa\nu' = -\beta \sin(\theta) - \gamma \cos(\theta), \tag{2.37}$$

$$\theta' = \nu, \tag{2.38}$$

$$y' = \sin(\theta), \tag{2.39}$$

with boundary conditions

$$\gamma(0) = \gamma(L) = 0, \nu(0) = \nu(L) = 0. \tag{2.40}$$

CHAPTER III

RESCALING THE ENERGY EQUATION

We wish to rescale this equation such that we can simplify the problem for analysis. Table 3.1 lists all the variables and parameters in the problem and lists the dimension of each. Next we derive the dimensions listed in Table 3.1. First of all, we know a few from the context of the problem, so we will fill them in now. We let F denote the dimension of force and L denote the dimension of length. From the derivation of total energy, we have that

$$\frac{dx}{ds} = \theta, \tag{3.1}$$

which implies that

$$\left[\frac{dx}{ds}\right] = \frac{[L]}{[L]} = 1 = [\theta]. \tag{3.2}$$

So θ is dimensionless.

By properties of dimensions, we also know that every term in the energy equation has equivalent dimensions. Therefore, since one term is βx and

$$[\beta][x] = FL, \tag{3.3}$$

we know that all terms have a dimension of force times length. Let us now look at

$$\frac{\kappa}{2}\int_0^L [\theta'(s)]^2 ds. \tag{3.4}$$

When we want the dimension but need to integrate a quantity, we take the dimension of the integrand times the dimension of the variable of integration. In this case, the term becomes

$$FL = [\kappa][\theta']^2[s], \tag{3.5}$$

$$FL = [\kappa](1/L)^2 L. \tag{3.6}$$

So we see $[\kappa] = FL^2$.

Looking at

$$\int_0^L \gamma_1(s)[y'(s) - \sin(\theta(s))]ds, \tag{3.7}$$

we follow the computation

$$FL = [\gamma_1][y'][s], \tag{3.8}$$

$$FL = [\gamma_1][L], \tag{3.9}$$

to see $[\gamma_1] = F$. Following a similar computation, we get that $[\gamma_2] = F$. Let us now look at Table 3.1.

Table 3.1: Table for rescaling total energy equation.

Vars/Params	Dimensions
E	FL
x	L
y	L
θ	1
s	L
κ	FL^2
V	F
D	L
γ_1	F
γ_2	F
β	F
ω	F
σ	L

With the completed table, we can now define rescaled variables. For this problem, we will rescale by the length of the graphene sheet, L. We rescale the variables as the following,

$$\hat{s} = \frac{s}{L}, \tag{3.10}$$

$$\hat{y} = \frac{y}{L}, \tag{3.11}$$

$$\hat{x} = \frac{x}{L}. \tag{3.12}$$

Now we will rescale term by term. Start with

$$\frac{\kappa}{2}\int_0^L (\theta'(s))^2 ds. \tag{3.13}$$

We first need to relate derivatives. If we set $\hat{\theta} = \theta$, then we get

$$\frac{d\hat{\theta}}{d\hat{s}} = \frac{d(\theta)}{d(s/L)} = L\frac{d\theta}{ds}, \tag{3.14}$$

or

$$\frac{1}{L}\hat{\theta}' = \theta'. \tag{3.15}$$

Also

$$d\hat{s} = \frac{1}{L}ds. \tag{3.16}$$

Now substituting the rescalings into (3.13) we get,

$$\frac{\kappa}{2}\int_0^L (\theta'(s))^2 ds = \frac{\kappa}{2}\int_0^L (\frac{1}{L}\hat{\theta}'(s))^2 L d\hat{s} = \frac{\kappa}{2L}\int_0^1 (\hat{\theta}')^2 d\hat{s}. \tag{3.17}$$

Moving on to the next term,

$$\int_0^L V(y(s))ds. \tag{3.18}$$

We let $\hat{V}(\hat{y}) = V(y)$ and then substitute to get

$$\int_0^L V(y(s))ds = \int_0^1 \hat{V}(\hat{y})Ld\hat{s} = L\int_0^1 \hat{V}(\hat{y})d\hat{s}. \tag{3.19}$$

We must look inside (2.11) to see

$$\hat{V}(\hat{y}) = \omega \left(\left(\frac{\sigma}{L\hat{y}} \right)^9 - \left(\frac{\sigma}{L\hat{y}} \right)^3 \right), \tag{3.20}$$

where

$$\hat{\sigma} = \frac{\sigma}{L}. \tag{3.21}$$

Following a similar process for the term

$$\int_0^L V(D - y(s))ds, \tag{3.22}$$

we reach

$$\int_0^L V(D - y(s))ds = L \int_0^1 \hat{V}(\hat{D} - \hat{y})d\hat{s}, \tag{3.23}$$

where

$$\hat{D} = \frac{D}{L}. \tag{3.24}$$

Substituting the rescaled x into

$$-\beta x(0) + \beta x(L), \tag{3.25}$$

yields

$$-\beta L\hat{x}(0) + \beta L\hat{x}(1). \tag{3.26}$$

Next we consider

$$\int_0^L \gamma_1(s)[y'(s) - \sin(\theta(s))]ds. \tag{3.27}$$

We need to relate a derivative, so

$$\frac{d\hat{y}}{d\hat{s}} = \frac{d(y/L)}{d(s/L)} = \frac{dy}{ds}. \tag{3.28}$$

Then substituting in the rescalings, we end up with

$$\int_0^L \gamma_1(s)[y'(s) - \sin(\theta(s))]ds = \int_0^1 \gamma_1(s)[\hat{y}'(s) - \sin(\hat{\theta}(s))]Ld\hat{s} \tag{3.29}$$
$$= L\int_0^1 \gamma_1(s)[\hat{y}'(s) - \sin(\hat{\theta}(s))]d\hat{s}.$$

Following an analogous computation for the term with cosine yields

$$L\int_0^1 \gamma_2(s)[\hat{x}'(s) - \cos(\hat{\theta}(s))]d\hat{s}. \tag{3.30}$$

Then the expression for total energy becomes

$$E[\hat{x},\hat{y},\hat{\theta}] = \frac{\kappa}{2L}\int_0^1 (\hat{\theta}')^2 d\hat{s} + L\int_0^1 \hat{V}(\hat{y})ds + L\int_0^1 \hat{V}(\hat{D}-\hat{y})d\hat{s} \tag{3.31}$$
$$+ L\int_0^1 \gamma_1(s)[\hat{y}'(s) - \sin(\hat{\theta}(s))]d\hat{s} + L\int_0^1 \gamma_2(s)[\hat{x}'(s) - \cos(\hat{\theta}(s))]d\hat{s}$$
$$- \beta L\hat{x}(0) + \beta L\hat{x}(1).$$

Now we rescale ω inside V with

$$\hat{\omega} = \frac{\omega L^2}{\kappa}, \tag{3.32}$$

and β with

$$\hat{\beta} = \frac{\beta L^2}{\kappa}, \tag{3.33}$$

and γ_1 and γ_2 in the same fashion

$$\hat{\gamma}_1 = \frac{\gamma_1 L^2}{\kappa}. \tag{3.34}$$

Then the expression for total energy becomes

$$E[\hat{x},\hat{y},\hat{\theta}] = \frac{\kappa}{2L}\int_0^1 (\hat{\theta}')^2 d\hat{s} + \frac{\kappa}{L}\int_0^1 \hat{V}(\hat{y})ds + \frac{\kappa}{L}\int_0^1 \hat{V}(\hat{D}-\hat{y})d\hat{s} \tag{3.35}$$
$$+ \frac{\kappa}{L}\int_0^1 \hat{\gamma}_1[\hat{y}'(s) - \sin(\hat{\theta}(s))]d\hat{s} + \frac{\kappa}{L}\int_0^1 \hat{\gamma}_2(s)[\hat{x}'(s) - \cos(\hat{\theta}(s))]d\hat{s}$$
$$- \hat{\beta}\frac{\kappa}{L}\hat{x}(0) + \hat{\beta}\frac{\kappa}{L}\hat{x}(1).$$

So we can rescale E such that

$$\hat{E} = \frac{EL}{\kappa}, \tag{3.36}$$

and the rescaled expression for total energy becomes

$$\begin{aligned}\hat{E}[\hat{x}, \hat{y}, \hat{\theta}] =& \frac{1}{2}\int_0^1 (\hat{\theta}')^2 d\hat{s} + \int_0^1 \hat{V}(\hat{y}) ds + \int_0^1 \hat{V}(\hat{D} - \hat{y}) d\hat{s} \\ &+ \int_0^1 \hat{\gamma}_1[\hat{y}'(s) - \sin(\hat{\theta}(s))] d\hat{s} + \int_0^1 \hat{\gamma}_2(s)[\hat{x}'(s) - \cos(\hat{\theta}(s))] d\hat{s} \\ &- \hat{\beta}\hat{x}(0) + \hat{\beta}\hat{x}(1).\end{aligned} \tag{3.37}$$

Note that

$$\hat{V}(\hat{y}) = \omega\left(\left(\frac{\hat{\sigma}}{\hat{y}}\right)^9 - \left(\frac{\hat{\sigma}}{\hat{y}}\right)^3\right). \tag{3.38}$$

To save writing, we will drop the hats on the rescaled variables. This results in the following rescaled system that we use for the remainder of the paper

$$\gamma' = V'(y) - V'(D - y), \tag{3.39}$$

$$\nu' = -\beta \sin(\theta) - \gamma \cos(\theta), \tag{3.40}$$

$$\theta' = \nu, \tag{3.41}$$

$$y' = \sin(\theta), \tag{3.42}$$

with boundary conditions

$$\gamma(0) = \gamma(1) = 0, \nu(0) = \nu(1) = 0. \tag{3.43}$$

CHAPTER IV

CURVE OF FIRST BIFURCATION POINTS

4.1 Trivial Branch

To begin the bifurcation analysis, we identify a trivial branch of solutions that corresponds to the graphene sheet being flat and parallel to the substrates. We think of this as the unbuckled configuration. For the trivial branch, we know that $\bar{y}$ must be a constant. So let

$$\bar{y}(s) = c \quad \forall\, s \in [0,1]. \tag{4.1}$$

From (2.39) we have that

$$\bar{y}' = 0 = \sin(\bar{\theta}), \tag{4.2}$$

which tells us that $\bar{\theta}$ is a constant and is a multiple of 2π. We choose $\bar{\theta} = 0$. Using equation (2.38), this implies that $\bar{\nu} = 0$. Putting the fact that $\bar{\theta} = 0$, and $\bar{\nu} = 0$ into equation (2.37), we get the result that

$$\bar{\gamma}\cos(0) = 0, \tag{4.3}$$

which implies that $\bar{\gamma} = 0$. Now we reach equation (2.36)

$$V'(\bar{y}) - V'(D - \bar{y}) = 0. \tag{4.4}$$

Rearranging, and using the fact that $\bar{y} = c$ we are left with

$$V'(c) = V'(D - c). \tag{4.5}$$

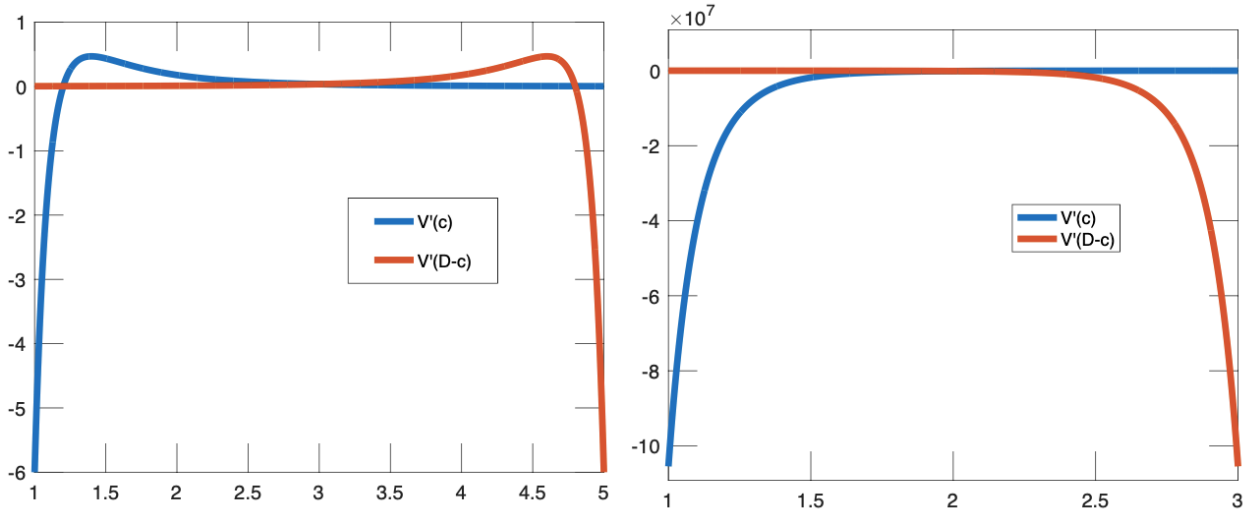

Figure 4.1: Plot for solutions of $V'(c)$ and $V'(D - c)$ showing three solutions vs one solution.

We notice that depending on if D is large or small, there is different solution behavior. For D larger than σ we get three solutions. The first solution occurs at $c = D/2$ while the other two solutions are similar and occur roughly σ away from where the plots tend to become large and negative. These two solutions occur because the rigid substrates are being pulled so far apart that the Van der Waals force from the further substrate becomes negligible and then the most natural location for the graphene layer to lay parallel and unbuckled occurs at the minimum energy location σ away from the closer substrate. For D smaller than σ we do not have the substrates

far enough apart for this phenomenon to occur and so there is only one solution at $c = D/2$.

For the trivial branch, we use the solution $c = D/2$ to (4.5). Thus the trivial branch is

$$\bar{\gamma} = 0, \tag{4.6}$$

$$\bar{\nu} = 0, \tag{4.7}$$

$$\bar{\theta} = 0, \tag{4.8}$$

$$\bar{y} = D/2, \tag{4.9}$$

for (2.36)-(2.39).

4.2 Linearizing the System

In order to compute the curve of first bifurcation points we need to find where the system changes from the unbuckled configuration to a buckled configuration. When we linearize, it will allow us to gain information about how the system behaves around the equilibrium solution that is the trivial branch. The bifurcation points will be nontrivial solutions to the linearized system around the trivial branch.

To linearize around the trivial branch, we substitute

$$\theta = \bar{\theta} + \epsilon\hat{\theta}, \tag{4.10}$$

$$\nu = \bar{\nu} + \epsilon\hat{\nu}, \tag{4.11}$$

$$\gamma = \bar{\gamma} + \epsilon\hat{\gamma}, \tag{4.12}$$

$$y = \bar{y} + \epsilon\hat{y}. \tag{4.13}$$

After these substitutions, we take $\frac{d}{d\epsilon}$ of both sides of each equation in (2.36)-(2.39) and then evaluate at $\epsilon = 0$. For equation (2.36) we have the following

$$\bar{\gamma}' + \epsilon\hat{\gamma}' = V'(\bar{y} + \epsilon\hat{y}) - V'(D - (\bar{y} + \epsilon\hat{y})). \tag{4.14}$$

Taking $\frac{d}{d\epsilon}$ of both sides

$$\frac{d}{d\epsilon}\left\{\bar{\gamma}' + \epsilon\hat{\gamma}'\right\} = \frac{d}{d\epsilon}\left\{V'(\bar{y} + \epsilon\hat{y}) - V'(D - (\bar{y} + \epsilon\hat{y}))\right\}, \tag{4.15}$$

or

$$\hat{\gamma}' = V''(\bar{y} + \epsilon\hat{y})(\hat{y}) - V''(D - (\bar{y} + \epsilon\hat{y}))(-\hat{y}). \tag{4.16}$$

Then setting $\epsilon = 0$ gives

$$\hat{\gamma}' = V''(\bar{y})(\hat{y}) + V''(D - \bar{y})(\hat{y}), \tag{4.17}$$

into which we substitute $\bar{y} = D/2$ to get

$$\hat{\gamma}' = V''(D/2)(\hat{y}) + V''(D - (D/2))(\hat{y}) = 2V''(D/2)\hat{y}. \tag{4.18}$$

For equation (2.37) we have the following

$$\bar{\nu}' + \epsilon\hat{\nu}' = -\beta\sin(\bar{\theta} + \epsilon\hat{\theta}) - (\bar{\gamma} + \epsilon\hat{\gamma})\cos(\bar{\theta} + \epsilon\hat{\theta}). \tag{4.19}$$

Taking $\frac{d}{d\epsilon}$ of both sides

$$\frac{d}{d\epsilon}\left\{\bar{\nu}' + \epsilon\hat{\nu}'\right\} = \frac{d}{d\epsilon}\left\{-\beta\sin(\bar{\theta} + \epsilon\hat{\theta}) - (\bar{\gamma} + \epsilon\hat{\gamma})\cos(\bar{\theta} + \epsilon\hat{\theta})\right\}, \tag{4.20}$$

or

$$\hat{\nu}' = -\beta\cos(\bar{\theta}+\epsilon\hat{\theta})(\hat{\theta}) - (\hat{\gamma}\cos(\bar{\theta}+\epsilon\hat{\theta}) - (\bar{\gamma}+\epsilon\hat{\gamma})\sin(\bar{\theta}+\epsilon\hat{\theta})(\hat{\theta})). \tag{4.21}$$

Then setting $\epsilon = 0$ gives

$$\hat{\nu}' = -\beta\cos(\bar{\theta})(\hat{\theta}) - (\hat{\gamma}\cos(\bar{\theta}) - (\bar{\gamma})\sin(\bar{\theta})(\hat{\theta})), \tag{4.22}$$

into which we substitute $\bar{\gamma} = 0$ and $\bar{\theta} = 0$ to get

$$\hat{\nu}' = -\beta\hat{\theta} - \hat{\gamma}. \tag{4.23}$$

For equation (2.38) we have the following

$$\bar{\theta}' + \epsilon\hat{\theta}' = \bar{\nu} + \epsilon\hat{\nu}. \tag{4.24}$$

Taking $\frac{d}{d\epsilon}$ of both sides

$$\frac{d}{d\epsilon}\left\{\bar{\theta}' + \epsilon\hat{\theta}'\right\} = \frac{d}{d\epsilon}\left\{\bar{\nu} + \epsilon\hat{\nu}\right\}, \tag{4.25}$$

or

$$\hat{\theta}' = \hat{\nu}. \tag{4.26}$$

For equation (2.39) we have the following

$$\bar{y}' + \epsilon\hat{y}' = \sin(\bar{\theta}+\epsilon\hat{\theta}). \tag{4.27}$$

Taking $\frac{d}{d\epsilon}$ of both sides

$$\frac{d}{d\epsilon}\left\{\bar{y}' + \epsilon\hat{y}'\right\} = \frac{d}{d\epsilon}\left\{\sin(\bar{\theta}+\epsilon\hat{\theta})\right\}, \tag{4.28}$$

or

$$\hat{y}' = \cos(\bar{\theta}+\epsilon\hat{\theta})(\hat{\theta}). \tag{4.29}$$

Then setting $\epsilon = 0$ gives

$$\hat{y}' = \cos(\bar{\theta})(\hat{\theta}), \tag{4.30}$$

into which we substitute $\bar{\theta} = 0$ to get

$$\hat{y}' = \hat{\theta}. \tag{4.31}$$

We also need to linearize the boundary conditions (2.40).

Computing

$$\frac{d}{d\epsilon}\left[(\bar{\nu} + \epsilon\hat{\nu})(0)\right]_{\epsilon=0} = \frac{d}{d\epsilon}\left[(\bar{\nu} + \epsilon\hat{\nu})(1) = 0\right]_{\epsilon=0}, \tag{4.32}$$

$$\frac{d}{d\epsilon}\left[(\bar{\gamma} + \epsilon\hat{\gamma})(0)\right]_{\epsilon=0} = \frac{d}{d\epsilon}\left[(\bar{\gamma} + \epsilon\hat{\gamma})(1) = 0\right]_{\epsilon=0}, \tag{4.33}$$

gives

$$\hat{\nu}(0) = \hat{\nu}(1) = 0, \tag{4.34}$$

and

$$\hat{\gamma}(0) = \hat{\gamma}(1) = 0. \tag{4.35}$$

Assembling the results of the above computations, we get the linear system

$$\hat{\gamma}' = 2V''(D/2)\hat{y}, \tag{4.36}$$

$$\hat{\nu}' = -\beta\hat{\theta} - \hat{\gamma}, \tag{4.37}$$

$$\hat{\theta}' = \hat{\nu}, \tag{4.38}$$

$$\hat{y}' = \hat{\theta}, \tag{4.39}$$

with boundary conditions

$$\hat{\nu}(0) = \hat{\nu}(1) = 0, \tag{4.40}$$

$$\hat{\gamma}(0) = \hat{\gamma}(1) = 0. \tag{4.41}$$

4.3 Transformation into a Single Equation

As mentioned in the previous section, we hope to find nontrivial solutions of this linearized system. All that remains now is to find points where the linear system (4.36)-(4.39) equals 0. In order to solve this system in a more direct manner, we convert this system into a single fouth-order linear differential to which we can apply elementary techniques.

The next task is to convert this linear system of differential equations into a single fourth-order linear differential equations with boundary conditions. We also drop the hats in this equation for sake of writing. We know that $\theta' = \nu$, so therefore $\theta'' = \nu'$. From equation (4.38) we have

$$\theta'' = \nu' = -\beta\theta - \gamma, \tag{4.42}$$

which implies that

$$\theta''' = -\beta\theta' - \gamma'. \tag{4.43}$$

Next using equation (4.37) we have

$$\theta''' = -\beta\theta' - \gamma' = -\beta\theta' - 2V''(D/2)y, \tag{4.44}$$

so that

$$\theta'''' = -\beta\theta'' - 2V''(D/2)y' - \beta\theta'' - 2V''(D/2)\theta, \tag{4.45}$$

where the second equality uses equation (4.39). We conclude that

$$\theta^{(4)} + \beta\theta'' + 2V''(D/2)\theta = 0. \tag{4.46}$$

Transforming the first boundary condition using equation (4.38) we see

$$\theta'(0) = \theta'(1) = 0. \tag{4.47}$$

Rearranging equation (4.37), we get

$$\gamma = -\beta\theta - \nu'. \tag{4.48}$$

And using equation (4.38) gives

$$\gamma = -\beta\theta - \theta''. \tag{4.49}$$

Therefore by (4.41) we get the additional boundary condition

$$-(\beta\theta + \theta'')(0) = -(\beta\theta + \theta'')(1) = 0. \tag{4.50}$$

Combining (4.46), (4.47), and (4.50), we reach the fourth-order linear equation with boundary conditions

$$\theta^{(4)} + \beta\theta'' + 2V''(D/2)\theta = 0, \tag{4.51}$$

$$\theta'(0) = \theta'(1) = 0, \tag{4.52}$$

$$\beta\theta(0) + \theta''(0) = \beta\theta(1) + \theta''(1) = 0. \tag{4.53}$$

4.4 Solving the 2-point bvp

As previously stated, the goal of solving this 2-point bvp is to find bifurcation points that are characterized as nontrivial solutions of the equations (4.51).

To begin solving (4.51)-(4.53), we will first rename the coefficient of θ. Let $\alpha = 2V''(D/2)$. Now the auxiliary equation for (4.51) is

$$m^4 + \beta m^2 + \alpha = 0. \tag{4.54}$$

This is a biquadratic, so if we make the substitution $u = m^2$ then it becomes

$$u^2 + \beta u + \alpha = 0. \tag{4.55}$$

Using the quadratic formula, we get

$$u = \frac{-\beta \pm \sqrt{\beta^2 - 4\alpha}}{2}. \tag{4.56}$$

Hence

$$m = \pm\sqrt{\frac{-\beta \pm \sqrt{\beta^2 - 4\alpha}}{2}}. \tag{4.57}$$

So (4.54) has the four roots

$$m_1 = \sqrt{\frac{-\beta + \sqrt{\beta^2 - 4\alpha}}{2}}, \tag{4.58}$$

$$m_2 = \sqrt{\frac{-\beta - \sqrt{\beta^2 - 4\alpha}}{2}}, \tag{4.59}$$

$$m_3 = -\sqrt{\frac{-\beta + \sqrt{\beta^2 - 4\alpha}}{2}}, \tag{4.60}$$

$$m_4 = -\sqrt{\frac{-\beta - \sqrt{\beta^2 - 4\alpha}}{2}}. \tag{4.61}$$

Because the boundary conditions are periodic, we want the roots to be pure imaginary numbers. Since both β and α are positive, a sufficient condition for this is that $\beta^2 - 4\alpha > 0$. After assuming this, it follows that the solution can be written as

$$\theta(s) = c_1 e^{m_1 s} + c_2 e^{m_2 s} + c_3 e^{m_3 s} + c_4 e^{m_4 s}, \tag{4.62}$$

where c_1 to c_4 are arbitrary constants.

Now we need to apply the boundary conditions (4.52) and (4.53) to the general solution. To do this, we need to compute the first two derivatives of (4.62). These are

$$\theta'(s) = c_1 m_1 e^{m_1 s} + c_2 m_2 e^{m_2 s} + c_3 m_3 e^{m_3 s} + c_4 m_4 e^{m_4 s}, \tag{4.63}$$

$$\theta''(s) = c_1 (m_1)^2 e^{m_1 s} + c_2 (m_2)^2 e^{m_2 s} + c_3 (m_3)^2 e^{m_3 s} + c_4 (m_4)^2 e^{m_4 s}. \tag{4.64}$$

Substituting these into (4.52) we get

$$\theta'(0) = c_1 m_1 + c_2 m_2 + c_3 m_3 + c_4 m_4 = 0, \tag{4.65}$$

$$\theta'(1) = c_1 m_1 e^{m_1} + c_2 m_2 e^{m_2} + c_3 m_3 e^{m_3} + c_4 m_4 e^{m_4} = 0. \tag{4.66}$$

Also, substituting into (4.53) we get

$$\beta\theta(0) + \theta''(0) = \beta(c_1 + c_2 + c_3 + c_4) + c_1 m_1^2 + c_2 m_2^2 + c_3 m_3^2 + c_4 m_4^2 = 0, \tag{4.67}$$

$$\begin{aligned} \beta\theta(1) + \theta''(1) = \beta(c_1 e^{m_1} + c_2 e^{m_2} + c_3 e^{m_3} + c_4 e^{m_4}) \\ + c_1 m_1^2 e^{m_1} + c_2 m_2^2 e^{m_2} + c_3 m_3^2 e^{m_3} + c_4 m_4^2 e^{m_4} = 0. \end{aligned} \tag{4.68}$$

This gives us a system of 4 linear equations for the coefficients c_1 to c_4. This system corresponds to the matrix equation

$$\begin{bmatrix} m_1 & m_2 & m_3 & m_4 \\ m_1 e^{m_1} & m_2 e^{m_2} & m_3 e^{m_3} & m_4 e^{m_4} \\ \beta + m_1^2 & \beta + m_2^2 & \beta + m_3^2 & \beta + m_4^2 \\ (\beta + m_1^2)e^{m_1} & (\beta + m_2^2)e^{m_2} & (\beta + m_3^2)e^{m_3} & (\beta + m_4^2)e^{m_4} \end{bmatrix} \begin{bmatrix} c_1 \\ c_2 \\ c_3 \\ c_4 \end{bmatrix} = \vec{0} \qquad (4.69)$$

We will now use this system and Matlab to numerically find the curve of first bifurcation points for different values of the parameters. Using Matlab we find the first location where the modulus of the determinant of (4.4) equals zero. This is equivalent to finding where the fourth-order linear differential equation (4.51) has nontrivial solutions and these will be the first bifurcation points. Using Matlab, we compute the modulus of the determinant of (4.4) for a mesh of points to determine the first time this curve hits the s-axis. We use the Matlab function *islocalmin* to determine where in the mesh of points the determinant has a local minimum. This avoids searching for an exact zero value where the computer may not be exactly zero. Then using the Matlab function *find*, we parse the logical array produced by *islocalmin* to find the first instance of a 1 which corresponds to a local minimum of the determinant of (4.4).

Once we have these solutions, we must remember that we set $\alpha = 2V''(D/2)$. Because of how (4.4) is set up, we have only found the alpha values and not the actual D values of the bifurcation points we are searching for. To fix this, we can

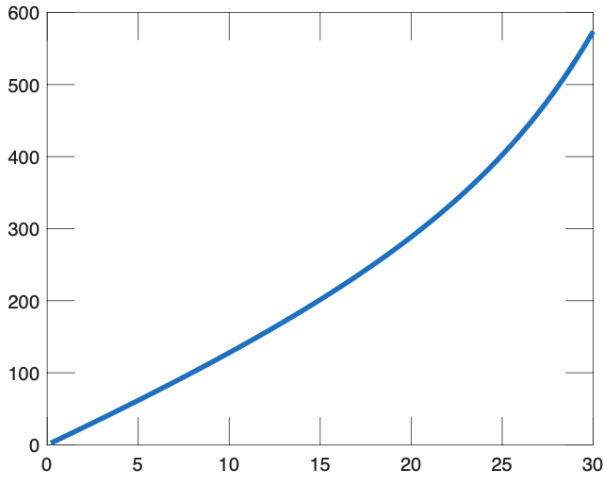

Figure 4.2: Example plot produced from the code in Appendix A showing the plot α vs β.

rewrite the equation $\alpha = 2V''(D/2)$ as a polynomial in terms of an unknown D with parameters ω and σ. Fixing these parameters, we can use the Matlab function *roots* in conjunction with *imag* to locate the real zero of this polynomial, which gives us the D values of the bifurcation points. Computing these values over a range of β values yields the curve of first bifurcation points.

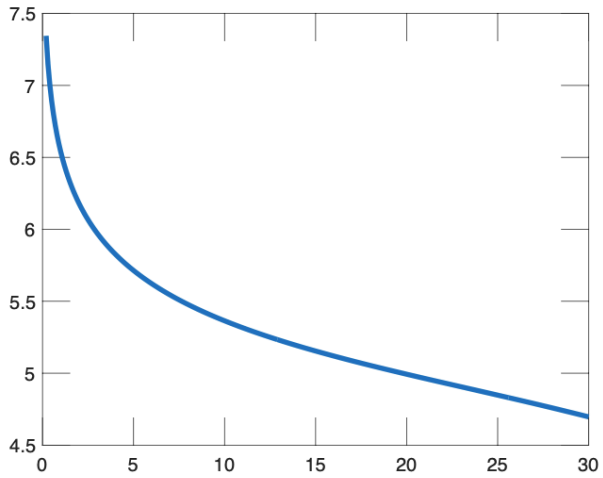

Figure 4.3: Example plot produced from the code in Appendix A showing the plot of first bifurcation points for the parameters $\sigma = 3, \omega = 2$.

CHAPTER V

ASYMPTOTICS

The main goal of this chapter concerning asymptotics is to describe the bifurcating branches near the bifurcation points resulting from the 2-point boundary value problem. Because the nonlinear 2-point boundary value problem cannot be solved analytically, we approximate solutions using expansions of the variables. Let ϵ be a small parameter. We also let the bifurcating branches be described parametrically by

$$\epsilon \mapsto (D(\epsilon), \vec{u}(\epsilon)), \tag{5.1}$$

and

$$\vec{u}(\epsilon) = [\theta(\epsilon), \nu(\epsilon), \gamma(\epsilon), y(\epsilon)]^T. \tag{5.2}$$

Assume $D(0) = \bar{D}$ and $\vec{u}(0) = \vec{0}$. Assume also that $D(\epsilon)$ and $\vec{u}(\epsilon)$ can be expanded in Taylor series near $\epsilon = 0$. So

$$D(\epsilon) = D_0 + D_1\epsilon + D_2\epsilon^2 + ..., \tag{5.3}$$

$$\theta(\epsilon) = \theta_0 + \theta_1\epsilon + \theta_2\epsilon^2 + ..., \tag{5.4}$$

$$\nu(\epsilon) = \nu_0 + \nu_1\epsilon + \nu_2\epsilon^2 + ..., \tag{5.5}$$

$$\gamma(\epsilon) = \gamma_0 + \gamma_1\epsilon + \gamma_2\epsilon^2 + ..., \tag{5.6}$$

$$y(\epsilon) = y_0 + y_1\epsilon + y_2\epsilon^2 + ..., \tag{5.7}$$

and we note that the expanded quantities of θ, ν, γ, y depend on both ϵ and s however when deriving these equations we suppress the s dependence to save space. We now plug (5.3)-(5.7) into (3.39)-(3.43) and equate like powers of ϵ.

5.1 Deriving the $\mathcal{O}(1)$ System

Plugging the expansions into (3.39)-(3.43) we have

$$\theta'(\epsilon) = \nu(\epsilon), \tag{5.8}$$

$$\nu'(\epsilon) = -\beta \sin(\theta(\epsilon)) - \gamma(\epsilon)\cos(\theta(\epsilon)), \tag{5.9}$$

$$\gamma'(\epsilon) = V'(y(\epsilon)) - V'(D(\epsilon) - y(\epsilon)), \tag{5.10}$$

$$y'(\epsilon) = \sin(\theta(\epsilon)). \tag{5.11}$$

At $\epsilon = 0$ we have

$$\theta_0' = \nu_0, \tag{5.12}$$

$$\nu_0' = -\beta \sin(\theta_0) - \gamma_0 \cos(\theta_0), \tag{5.13}$$

$$\gamma_0' = V'(y_0) - V'(D_0 - y_0), \tag{5.14}$$

$$y_0' = \sin(\theta_0), \tag{5.15}$$

with boundary conditions

$$\gamma_0(0) = \gamma_0(1) = 0, \tag{5.16}$$

$$\nu_0(0) = \nu_0(1) = 0. \tag{5.17}$$

Note that this system is satisfied by the base states which must happen since we have chosen to expand about said base states.

5.2 Deriving the $\mathcal{O}(\epsilon)$ System

Now we continue on to the $\mathcal{O}(\epsilon)$ system. To derive the $\mathcal{O}(\epsilon)$ system, we need to compute the derivative with respect to ϵ of both sides of each equation in (5.8)-(5.11). We get

$$\theta'_\epsilon(\epsilon) = \nu_\epsilon(\epsilon), \tag{5.18}$$

$$\nu'_\epsilon(\epsilon) = -\beta\cos(\theta(\epsilon))\theta_\epsilon(\epsilon) - \gamma_\epsilon(\epsilon)\cos(\theta(\epsilon)) + \sin(\theta(\epsilon))\theta_\epsilon(\epsilon)\gamma(\epsilon), \tag{5.19}$$

$$\gamma'_\epsilon(\epsilon) = V''(y(\epsilon))y_\epsilon(\epsilon) - V''(D(\epsilon) - y(\epsilon))(D_\epsilon(\epsilon) - y_\epsilon(\epsilon)), \tag{5.20}$$

$$y'_\epsilon(\epsilon) = \cos(\theta(\epsilon))\theta_\epsilon(\epsilon). \tag{5.21}$$

Evaluating at $\epsilon = 0$ we have

$$\theta'_1 = \nu_1, \tag{5.22}$$

$$\nu'_1 = -\beta\cos(\theta_0)\theta_1 - \gamma_1\cos(\theta_0) + \sin(\theta_0)\theta_1\gamma_0, \tag{5.23}$$

$$\gamma'_1 = V''(y_0)y_1 - V''(D_0 - y_0)(D_1 - y_1), \tag{5.24}$$

$$y'_1 = \cos(\theta_0)\theta_1. \tag{5.25}$$

Plugging in the base states gives

$$\theta_1' = \nu_1, \tag{5.26}$$

$$\nu_1' = -\beta\theta_1 - \gamma_1, \tag{5.27}$$

$$\gamma_1' = 2V''(D/2)y_1 - V''(D/2)D_1, \tag{5.28}$$

$$y_1' = \theta_1. \tag{5.29}$$

And it is clear that the boundary conditions for the $\mathcal{O}(\epsilon)$ problem are

$$\gamma_1(0) = \gamma_1(1) = 0, \tag{5.30}$$

$$\nu_1(0) = \nu_1(1) = 0. \tag{5.31}$$

So the $\mathcal{O}(\epsilon)$ system is (5.26)-(5.29) with boundary conditions (5.30), (5.31).

5.3 Deriving the $\mathcal{O}(\epsilon^2)$ System

Now we continue on to the $\mathcal{O}(\epsilon^2)$ system. To derive the $\mathcal{O}(\epsilon^2)$ system, we must again compute the derivative with respect to ϵ of both sides of each equation in (5.18)-(5.21). We get

$$\theta'_{\epsilon\epsilon}(\epsilon) = \nu_{\epsilon\epsilon}(\epsilon), \tag{5.32}$$

$$\begin{aligned}\nu'_{\epsilon\epsilon}(\epsilon) = {} & \beta \sin(\theta(\epsilon))\theta_\epsilon(\epsilon)^2 - \theta_{\epsilon\epsilon}(\epsilon)\beta\cos(\theta(\epsilon)) - \gamma_{\epsilon\epsilon}(\epsilon)\cos(\theta(\epsilon)) \\ & + \gamma_\epsilon(\epsilon)\theta_\epsilon(\epsilon)\sin(\theta(\epsilon)) + \gamma(\epsilon)\theta_\epsilon(\epsilon)^2\cos(\theta(\epsilon)) \\ & + \sin(\theta(\epsilon))\theta_{\epsilon\epsilon}(\epsilon)\gamma(\epsilon) + \gamma_\epsilon(\epsilon)\theta_\epsilon(\epsilon)\sin(\theta(\epsilon)),\end{aligned} \tag{5.33}$$

$$\begin{aligned}\gamma'_{\epsilon\epsilon}(\epsilon) = {} & V'''(y(\epsilon))y_\epsilon(\epsilon)^2 + V''(y(\epsilon))y_{\epsilon\epsilon}(\epsilon) - V'''(D(\epsilon) - y(\epsilon))(D_\epsilon(\epsilon) \\ & - y_\epsilon(\epsilon))^2 - V''(D(\epsilon) - y(\epsilon))(D_{\epsilon\epsilon}(\epsilon) - y_{\epsilon\epsilon}(\epsilon)),\end{aligned} \tag{5.34}$$

$$y'_{\epsilon\epsilon}(\epsilon) = -\sin(\theta(\epsilon))\theta_\epsilon(\epsilon)^2 + \theta_{\epsilon\epsilon}(\epsilon)\cos(\theta(\epsilon)). \tag{5.35}$$

Evaluating at $\epsilon = 0$ we have

$$2\theta'_2 = 2\nu_2, \tag{5.36}$$

$$\begin{aligned}2\nu'_2 = {} & \beta\sin(\theta_0)\theta_1^2 - 2\theta_2\beta\cos(\theta_0) - 2\gamma_2\cos(\theta_0) \\ & + \gamma_1\theta_1\sin(\theta_0) + \gamma_0\theta_1^2\cos(\theta_0) + 2\sin(\theta_0)\theta_2\gamma_0 + \gamma_1\theta_1\sin(\theta_0),\end{aligned} \tag{5.37}$$

$$\begin{aligned}2\gamma'_2 = {} & V'''(y_0)y_1^2 + 2V''(y_0)y_2 - V'''(D_0 - y_0)(D_1 - y_1)^2 \\ & - V''(D_0 - y_0)(2D_2 - 2y_2),\end{aligned} \tag{5.38}$$

$$2y'_2 = -\sin(\theta_0)\theta_1^2 + 2\theta_2\cos(\theta_0). \tag{5.39}$$

Plugging in the base states gives

$$\theta_2' = \nu_2, \tag{5.40}$$

$$\nu_2' = -\beta\theta_2 - \gamma_2, \tag{5.41}$$

$$\gamma_2' = 2V''(D/2)y_2 - V''(D/2)D_2 - \frac{1}{2}V'''(D/2)(D_1^2 - 2D_1y_1), \tag{5.42}$$

$$y_2' = \theta_2. \tag{5.43}$$

And it is clear that the boundary conditions for the $\mathcal{O}(\epsilon^2)$ problem are

$$\gamma_2(0) = \gamma_2(1) = 0, \tag{5.44}$$

$$\nu_2(0) = \nu_2(1) = 0. \tag{5.45}$$

So the $\mathcal{O}(\epsilon^2)$ system is (5.40)-(5.43) with boundary conditions (5.44), (5.45).

5.4 Deriving the $\mathcal{O}(\epsilon^3)$ System

Now we continue on to the $\mathcal{O}(\epsilon^3)$ system. To derive the $\mathcal{O}(\epsilon^3)$ system, we must again compute the derivative with respect to ϵ of both sides of each equation in (5.32)-(5.35). To save writing we suppress the ϵ dependence on the variables below resulting in

$$\theta'_{\epsilon\epsilon\epsilon} = \nu_{\epsilon\epsilon\epsilon}, \tag{5.46}$$

$$\begin{aligned}\nu'_{\epsilon\epsilon\epsilon} = {} & \beta\cos(\theta)\theta_\epsilon^3 + 2\beta\sin(\theta)\theta_\epsilon\theta_{\epsilon\epsilon} - \theta_{\epsilon\epsilon\epsilon}\beta\cos(\theta) + \theta_{\epsilon\epsilon}\beta\theta_\epsilon\sin(\theta) \\ & - \gamma_{\epsilon\epsilon\epsilon}\cos(\theta) + \gamma_{\epsilon\epsilon}\sin(\theta)\theta_\epsilon + [\gamma_{\epsilon\epsilon}\theta_\epsilon + \theta_{\epsilon\epsilon}\gamma_\epsilon]\sin(\theta) + \gamma_\epsilon\theta_\epsilon^2\cos(\theta) \\ & + [2\theta_\epsilon\theta_{\epsilon\epsilon}\gamma + \gamma_\epsilon\theta_\epsilon^2]\cos(\theta) - \gamma\theta_\epsilon^3\sin(\theta) \\ & + [\theta_{\epsilon\epsilon\epsilon}\gamma + 2\gamma_\epsilon\theta_{\epsilon\epsilon} + \gamma_{\epsilon\epsilon}\theta_\epsilon]\sin(\theta) + \cos(\theta)\theta_\epsilon[\theta_{\epsilon\epsilon}\gamma + \gamma_\epsilon\theta_\epsilon],\end{aligned} \tag{5.47}$$

$$\begin{aligned}\gamma'_{\epsilon\epsilon\epsilon} = {} & V''''(y)y_\epsilon^3 + 3y_\epsilon y_{\epsilon\epsilon}V'''(y) + V''(y)y_{\epsilon\epsilon\epsilon} - V''''(D-y)(D_\epsilon - y_\epsilon)^3 \\ & - 3(D_\epsilon - y_\epsilon)(D_{\epsilon\epsilon} - y_{\epsilon\epsilon})V'''(D-y) - V''(D-y)(D_{\epsilon\epsilon\epsilon} - y_{\epsilon\epsilon\epsilon}),\end{aligned} \tag{5.48}$$

$$y'_{\epsilon\epsilon\epsilon} = -\cos(\theta)\theta_\epsilon^3 - 2\theta_\epsilon\theta_{\epsilon\epsilon}\sin(\theta) + \theta_{\epsilon\epsilon\epsilon}\cos(\theta) - \theta_{\epsilon\epsilon}\theta_\epsilon\sin(\theta). \tag{5.49}$$

Evaluating at $\epsilon = 0$ we have

$$6\theta'_3 = 6\nu_3, \tag{5.50}$$

$$6\nu'_3 = \beta\theta_1^3 - 6\theta_3\beta - 6\gamma_3 + \gamma_1\theta_1^2 + \gamma_1\theta_1^2 + \gamma_1\theta_1^2, \tag{5.51}$$

$$\begin{aligned}6\gamma'_3 = {} & V''''(D/2)y_1^3 + 6y_1y_2V'''(D/2) + 6y_3V''(D/2) - V''''(D/2)(D_1 - y_1)^3 \\ & - 3(D_1 - y_1)(2D_2 - 2y_2)V'''(D/2) - V''(D/2)(6D_3 - 6y_3),\end{aligned} \tag{5.52}$$

$$6y'_3 = -\theta_1^3 + 6\theta_3. \tag{5.53}$$

Plugging in the base states gives

$$\theta_3' = \nu_3, \tag{5.54}$$

$$\nu_3' = -\beta\theta_3 - \gamma_3 + \frac{\beta}{6}\theta_1^3 + \frac{\gamma_1\theta_1^2}{2}, \tag{5.55}$$

$$\begin{aligned}\gamma_3' = {} & 2V''(D/2)y_3 - V''(D/2)D_3 + \frac{1}{6}V''''(D/2)(y_1^3 - (D_1 - y_1)^3) \\ & + V'''(D/2)(y_1y_2 - (D_1 - y_1)(D_2 - y_2)),\end{aligned} \tag{5.56}$$

$$y_3' = \theta_3 - \frac{\theta_1^3}{6}. \tag{5.57}$$

And it is clear that the boundary conditions for the $\mathcal{O}(\epsilon^3)$ problem are

$$\gamma_3(0) = \gamma_3(1) = 0, \tag{5.58}$$

$$\nu_3(0) = \nu_3(1) = 0. \tag{5.59}$$

So the $\mathcal{O}(\epsilon^3)$ system is (5.54)-(5.57) with boundary conditions (5.58), (5.59).

CHAPTER VI

SOLVABILITY CONDITIONS AND ASYMPTOTIC SYSTEMS

In order to gain information about the expansion for the bifurcation parameter (5.3) we need to use the systems found in the previous chapter. Because some of these systems can be too difficult to solve, we will need to use the Fredholm Alternative Theorem to gain information. To apply this theorem, we convert each system to single differential equation.

6.1 Converting Systems to a Single Fourth-Order ODE

The process of converting the systems to a single equation is analogous to what we did to get equation (4.51). Note that each of the systems (5.26)-(5.31), (5.40)-(5.45), and (5.54)-(5.59) has the structure

$$\theta_i' = \nu_i + H_0, \tag{6.1}$$

$$\nu_i' = -\beta\theta_i - \gamma_i + H_1, \tag{6.2}$$

$$\gamma_i' = 2V''(D/2)y_i - V''(D/2)D_i + H_2, \tag{6.3}$$

$$y_i' = \theta_i + H_3, \tag{6.4}$$

with

$$\gamma_i(0) = \gamma_i(1) = 0, \tag{6.5}$$

$$\nu_i(0) = \nu_i(1) = 0, \tag{6.6}$$

where H_0 to H_3 depend on lower-order terms from the expansions.

We will convert this system into a single boundary-value problem for a fourth-order ODE. Using the Fredholm Alternative Theorem on the general case will allow us to find solvability conditions, which we can then apply to the specific systems (5.26)-(5.31), (5.40)-(5.45), and (5.54)-(5.59).

Differentiating (6.1) we get

$$\theta_i'' = \nu_i' + H_0'. \tag{6.7}$$

Solving this equation for ν_i' and substituting in equation (6.2) gives

$$\theta_i'' - H_0' = -\beta\theta_i - \gamma_i + H_1, \tag{6.8}$$

which after differentiating, gives

$$\theta_i''' - H_0'' = -\beta\theta_i' - \gamma_i' + H_1'. \tag{6.9}$$

Using equation (6.3) to replace γ_i' gives

$$\theta_i''' - H_0'' = -\beta\theta_i' - (2V''(D/2)y_i - V''(D/2)D_i + H_2) + H_1'. \tag{6.10}$$

Differentiating again gives

$$\theta_i'''' - H_0''' = -\beta\theta_i'' - 2V''(D/2)y_i' - H_2' + H_1''. \tag{6.11}$$

Lastly, we use equation (6.4) to replace y_i' to get

$$\theta_i'''' - H_0''' = -\beta\theta_i'' - 2V''(D/2)(\theta_i + H_3) - H_2' + H_1''. \tag{6.12}$$

Rearranging we are left with the fourth-order linear inhomogeneous equation

$$\theta_i'''' + \beta\theta_i'' + 2V''(D/2)\theta_i = H_0''' + H_1'' - H_2' - 2V''(D/2)H_3. \tag{6.13}$$

Next we derive the appropriate boundary conditions. For the $\mathcal{O}(\epsilon^i)$ system, the boundary conditions are

$$\gamma_i(0) = \gamma_i(1) = 0, \tag{6.14}$$

$$\nu_i(0) = \nu_i(1) = 0. \tag{6.15}$$

Using equation (6.1), we see that (6.15) becomes

$$\theta_i'(0) = H_0(0), \tag{6.16}$$

$$\theta_i'(1) = H_0(1). \tag{6.17}$$

Using equations (6.1) and (6.3), we see that (6.14) becomes

$$\beta\theta_i(0) + \theta_i''(0) = H_0'(0) + H_1(0), \tag{6.18}$$

$$\beta\theta_i(1) + \theta_i''(1) = H_0'(1) + H_1(1). \tag{6.19}$$

6.2 Finding a General Homogeneous Adjoint Problem

Next we derive a solvability condition for the general fourth-order linear differential equation that arises in each step of the asymptotics procedure. From the previous

section, this problem is

$$\theta'''' + \beta\theta'' + 2V''(D/2)\theta = H_0'''' + H_1'' - H_2' - 2V''(D/2)H_3, \tag{6.20}$$

$$\theta'(0) = H_0(0), \tag{6.21}$$

$$\theta'(1) = H_0(1), \tag{6.22}$$

$$\beta\theta(0) + \theta''(0) = H_0'(0) + H_1(0), \tag{6.23}$$

$$\beta\theta(1) + \theta''(1) = H_0'(1) + H_1(1). \tag{6.24}$$

Now let us denote the inhomogeneous part of the differential equation by

$$f(s) = H_0''' + H_1'' - H_2' - 2V''(D/2)H_3. \tag{6.25}$$

Let us define $A = 2V''(D/2)$ as well as

$$\gamma_1 = H_0(0), \tag{6.26}$$

$$\gamma_2 = H_0(1), \tag{6.27}$$

$$\gamma_3 = H_0'(0) + H_1(0), \tag{6.28}$$

$$\gamma_4 = H_0'(1) + H_1(1). \tag{6.29}$$

To derive the solvability condition, we apply Theorem 4.1 in Chapter 11 of [12]. To begin we first need to find the homogeneous adjoint problem. To do this, we need the adjoint operator as well as the adjoint boundary operators. To find these, we look at the integral form of Green's Formula. Let $\theta, v \in C^4([0,1])$.

Then

$$\int_0^1 (L\theta(x))v(x)dx = \int_0^1 (\theta'''' + \beta\theta'' + A\theta)vdx \tag{6.30}$$

$$= \int_0^1 \theta''''vdx + \int_0^1 \beta\theta''vdx + \int_0^1 A\theta vdx \tag{6.31}$$

$$= v\theta'''|_0^1 - \int_0^1 \theta'''v'dx + \beta v\theta'|_0^1 - \int_0^1 \beta\theta'v'dx + \int_0^1 A\theta vdx \tag{6.32}$$

$$= v\theta'''|_0^1 - v'\theta''|_0^1 + \int_0^1 \theta''v''dx + \beta v\theta'|_0^1 - \beta v'\theta|_0^1 \tag{6.33}$$

$$+ \int_0^1 \beta\theta v''dx + \int_0^1 A\theta vdx$$

$$= v\theta'''|_0^1 - v'\theta''|_0^1 + v''\theta'|_0^1 - v'''\theta|_0^1 + \int_0^1 \theta v''''dx \tag{6.34}$$

$$+ \beta v\theta'|_0^1 - \beta v'\theta|_0^1 + \int_0^1 \beta\theta v''dx + \int_0^1 A\theta vdx.$$

where we have performed integration by parts several times.

Grouping the integral terms back together we get

$$\int_0^1 (L\theta(x))v(x)dx = \int_0^1 \theta v'''' + \beta\theta v'' + A\theta vdx + v\theta'''|_0^1 - v'\theta''|_0^1 \tag{6.35}$$

$$+ v''\theta'|_0^1 - v'''\theta|_0^1 + \beta v\theta'|_0^1 - \beta v'\theta|_0^1$$

$$= \int_0^1 \theta(x)(L^*v(x))dx + v\theta'''|_0^1 - v'\theta''|_0^1 + v''\theta'|_0^1 - v'''\theta|_0^1 \tag{6.36}$$

$$+ \beta v\theta'|_0^1 - \beta v'\theta|_0^1 .$$

We have derived Green's Formula,

$$\int_0^1 (L\theta(x))v(x)dx = \int_0^1 \theta(x)(L^*v(x))dx + J(\theta, v)|_0^1 , \tag{6.37}$$

and we have verified that $L^* = L$, i.e. L is formally self-adjoint, and we have discovered that

$$J(\theta, v)|_0^1 = v\theta'''|_0^1 - v'\theta''|_0^1 + v''\theta'|_0^1 - v'''\theta|_0^1 + \beta v\theta'|_0^1 - \beta v'\theta|_0^1 . \tag{6.38}$$

We still need the adjoint boundary operators so we look at the conjoint $J(\theta, v)|_0^1$. See Theorem 2.1 in Chapter 11 of [12]. Assume θ satisfies the homogeneous version of the boundary conditions (6.23) and (6.24) for the probelm. Then the below conjoint becomes

$$J(\theta, v)|_0^1 = v\theta'''|_0^1 - v'\theta''|_0^1 + v''\theta'|_0^1 - v'''\theta|_0^1 + \beta v\theta'|_0^1 - \beta v'\theta|_0^1 \tag{6.39}$$

$$= v\theta'''|_0^1 - v'(1)\theta''(1) + v(0)\theta''(0) + v''(1)\theta'(1) - v''(0)\theta'(0) - v'''\theta|_0^1 \tag{6.40}$$

$$+ \beta v(1)\theta'(1) - \beta v(0)\theta'(0) - \beta v'(1)\theta(1) + \beta v'(0)\theta(0)$$

$$= v\theta'''|_0^1 - v'''\theta|_0^1 - v'(1)(\theta''(1) + \beta\theta(1)) + v'(0)(\theta''(0) + \beta\theta(0)) \tag{6.41}$$

$$= v\theta'''|_0^1 - v'''\theta|_0^1 \tag{6.42}$$

$$= v(1)\theta'''(1) - v(0)\theta'''(0) - v'''(1)\theta(1) + v'''(0)\theta(0). \tag{6.43}$$

The conjoint is 0, if we require that ν satisfies

$$v(1) = v(0) = v'''(1) = v'''(0) = 0, \tag{6.44}$$

which we therefore take as the conditions for the homogeneous adjoint problem. Together, the homogeneous adjoint problem becomes

$$v'''' + \beta v'' + Av = 0, \tag{6.45}$$

$$v(0) = v(1) = 0, \tag{6.46}$$

$$v'''(0) = v'''(1) = 0. \tag{6.47}$$

6.3 Solving the Homogeneous Adjoint Problem

To begin solving the homogeneous adjoint problem (6.45)-(6.47) we will follow the same method used to solve the original linearized system (4.51)-(4.53). The auxiliary equation becomes

$$m^4 + \beta m^2 + A = 0. \tag{6.48}$$

This is a biquadratic, so if we make the substitution $u = m^2$ then it becomes

$$u^2 + \beta u + A = 0. \tag{6.49}$$

Using the quadratic formula, we get

$$u = \frac{-\beta \pm \sqrt{\beta^2 - 4A}}{2}, \tag{6.50}$$

and reversing the substitution gives

$$m = \sqrt{\frac{-\beta \pm \sqrt{\beta^2 - 4A}}{2}}. \tag{6.51}$$

This gives us four roots

$$m_1 = \sqrt{\frac{-\beta + \sqrt{\beta^2 - 4A}}{2}}, \tag{6.52}$$

$$m_2 = \sqrt{\frac{-\beta - \sqrt{\beta^2 - 4A}}{2}}, \tag{6.53}$$

$$m_3 = -\sqrt{\frac{-\beta + \sqrt{\beta^2 - 4A}}{2}}, \tag{6.54}$$

$$m_4 = -\sqrt{\frac{-\beta - \sqrt{\beta^2 - 4A}}{2}}. \tag{6.55}$$

We assume $\beta^2 - 4A > 0$ and so the general solution is of the form

$$v(s) = c_1 e^{m_1 s} + c_2 e^{m_2 s} + c_3 e^{m_3 s} + c_4 e^{m_4 s}. \tag{6.56}$$

Now we need to apply the boundary conditions (6.46), (6.47). To do this, we need to compute the first three derivatives of (6.56). These are

$$v'(s) = c_1 m_1 e^{m_1 s} + c_2 m_2 e^{m_2 s} + c_3 m_3 e^{m_3 s} + c_4 m_4 e^{m_4 s}, \tag{6.57}$$

$$v''(s) = c_1 (m_1)^2 e^{m_1 s} + c_2 (m_2)^2 e^{m_2 s} + c_3 (m_3)^2 e^{m_3 s} + c_4 (m_4)^2 e^{m_4 s}, \tag{6.58}$$

$$v'''(s) = c_1 (m_1)^3 e^{m_1 s} + c_2 (m_2)^3 e^{m_2 s} + c_3 (m_3)^3 e^{m_3 s} + c_4 (m_4)^3 e^{m_4 s}. \tag{6.59}$$

Substituting in the boundary conditions we get

$$v(0) = c_1 + c_2 + c_3 + c_4 = 0, \tag{6.60}$$

$$v(1) = c_1 e^{m_1} + c_2 e^{m_2} + c_3 e^{m_3} + c_4 e^{m_4} = 0, \tag{6.61}$$

$$v'''(0) = c_1 (m_1)^3 + c_2 (m_2)^3 + c_3 (m_3)^3 + c_4 (m_4)^3 = 0, \tag{6.62}$$

$$v'''(1) = c_1 (m_1)^3 e^{m_1} + c_2 (m_2)^3 e^{m_2} + c_3 (m_3)^3 e^{m_3} + c_4 (m_4)^3 e^{m_4} = 0. \tag{6.63}$$

Now we suppose the system has a linearly independent solution $\bar{c}_1, \bar{c}_2, \bar{c}_3, \bar{c}_4$. We denote $\bar{v}$ as (6.56) with $\bar{c}_1, \bar{c}_2, \bar{c}_3, \bar{c}_4$ as the arbitrary coefficients.

Then let θ be a solution to (6.20) and $v = \alpha \bar{v}$, where alpha is a non-zero constant, be a solution to the homogeneous adjoint problem (6.45)-(6.47). Then inserting into (6.37) we have

$$\int_0^1 f(x) \alpha \bar{v}(x) dx = \int_0^1 \theta(x) (L^* \bar{v}(x)) dx + \alpha J(\theta, \bar{v})|_0^1 . \tag{6.64}$$

However since $\bar{v}$ is a solution to (6.45) we have

$$\int_0^1 f(x) \alpha \bar{v}(x) dx = \alpha J(\theta, \bar{v})|_0^1 = \alpha (\theta' \bar{v}'' - \theta'' \bar{v}' - \beta \theta \bar{v})|_0^1, \tag{6.65}$$

where the second equality because $\bar{v}$ satisfies the homogeneous adjoint problem. Then

$$\int_0^1 f(x)\bar{v}(x)dx = \theta'(1)\bar{v}''(1) - (\beta\theta(1) + \theta''(1))\bar{v}'(1) - \theta'(0)\bar{v}''(0) \tag{6.66}$$

$$+ (\beta\theta(0) + \theta''(0))\bar{v}'(0).$$

By substituting in the original boundary conditions, this becomes

$$\int_0^1 f(x)\bar{v}(x)dx = \gamma_2\bar{v}''(1) - \gamma_4\bar{v}'(1) - \gamma_1\bar{v}''(0) + \gamma_3\bar{v}'(0), \tag{6.67}$$

which is the solvability condition for the general problem (6.20)-(6.24).

6.4 Solvability for D_1

We now apply the solvability condition (6.67) to (5.40)-(5.43) in order to discover the coefficient D_1 in the expansion (5.3) for D. We know that $f(s)$ for the general solvability condition (6.67) is given by (6.25). To apply the solvability condition to the $\mathcal{O}(\epsilon^2)$ system, we note that for (5.40)-(5.43),

$$H_0 = 0, \tag{6.68}$$

$$H_1 = 0, \tag{6.69}$$

$$H_2 = -\frac{1}{2}V'''(D/2)(D_1^2 - 2D_1y_1), \tag{6.70}$$

$$H_3 = 0. \tag{6.71}$$

So the $f(s)$ for this system is

$$f(s) = -H_2'. \tag{6.72}$$

Differentiating H_2 we have

$$H_2' = V'''(D/2)D_1y_1'. \tag{6.73}$$

By (5.29) we know that $y_1' = \theta_1$. Also by (6.26)-(6.29) we have that $\gamma_1, \gamma_2, \gamma_3, \gamma_4$ are all zero. Then the solvability condition becomes

$$\int_0^1 V'''(D/2)D_1\theta_1\bar{v}(x)dx = 0. \tag{6.74}$$

Then

$$D_1 \int_0^1 \theta_1\bar{v}(x)dx = 0. \tag{6.75}$$

The integral here depends on the parameters ω, σ, and on β. In Chapter 7 below, when we do the parametric study, we compute this integral in specific cases and see that it is nonzero. Then for any such case, $D_1 = 0$.

6.5 Solvability for D_2

We now apply the solvability condition (6.67) to (5.54)-(5.57) in order to discover the coefficient D_2 in the expansion (5.3) for D. We know that $f(s)$ for the general solvability condition (6.67) is given by (6.25). To apply the solvability condition to the $\mathcal{O}(\epsilon^3)$ system, we note that for (5.54)-(5.57),

$$H_0 = 0, \tag{6.76}$$

$$H_1 = \frac{\beta}{6}\theta_1^3 + \frac{\gamma_1\theta_1^2}{2}, \tag{6.77}$$

$$H_2 = \frac{1}{6}V''''(D/2)(y_1^3 - (D_1 - y_1)^3) + V'''(D/2)(y_1y_2 - (D_1 - y_1)(D_2 - y_2)), \tag{6.78}$$

$$H_3 = -\frac{\theta_1^3}{6}. \tag{6.79}$$

In order to obtain the γ_i values from the solvability conditions (6.26)-(6.29) for the $\mathcal{O}(\epsilon^3)$ problem, we compute the derivatives of H_1, H_2, and H_3 that we need. For H_1

taking derivatives we get

$$H_1' = \frac{\beta}{2}\theta_1^2\theta_1' + \frac{1}{2}\gamma_1'\theta_1^2 + \gamma_1\theta_1\theta_1', \tag{6.80}$$

$$H_1'' = \beta\theta_1(\theta_1')^2 + \frac{\beta}{2}\theta_1^2\theta_1'' + \frac{1}{2}\gamma_1''\theta_1^2 + \gamma_1'\theta_1\theta_1' + \gamma_1'\theta_1\theta_1' + \gamma_1((\theta_1')^2 + \theta_1\theta_1''). \tag{6.81}$$

For H_2 we first use the assumption that $D_1 = 0$ to simplify to

$$H_2 = \frac{1}{3}V''''(D/2)y_1^3 + V'''(D/2)y_1D_2. \tag{6.82}$$

Now taking a derivative we get

$$H_2' = V''''(D/2)y_1^2y_1' + V'''(D/2)y_1'D_2. \tag{6.83}$$

Plugging (6.76), (6.81), (6.83), and (6.79) into (6.25) gives us

$$\begin{aligned} f(s) = {} & \beta\theta_1(\theta_1')^2 + \frac{\beta}{2}\theta_1^2\theta_1'' + \frac{1}{2}\gamma_1''\theta_1^2 + 2\gamma_1'\theta_1\theta_1' + \gamma_1(\theta_1')^2 \\ & + \gamma_1\theta_1\theta_1'' - V''''(D/2)y_1^2y_1' - V'''(D/2)y_1'D_2 + \frac{1}{3}V''(D/2)\theta_1^3. \end{aligned} \tag{6.84}$$

Now we must refer to the $\mathcal{O}(\epsilon)$ system to rewrite $f(s)$ in terms of θ_1 which is known. From this system (5.18)-(5.21) we have

$$\gamma_1 = -\beta\theta_1 - \theta_1'', \gamma_1' = -\beta\theta_1' - \theta_1''', \gamma_1'' = -\beta\theta_1'' - \theta_1'''', \tag{6.85}$$

$$y_1 = \frac{-\beta\theta_1' - \theta_1'''}{2V''(D/2)}. \tag{6.86}$$

Substituting these identities into $f(s)$ above gives

$$\begin{aligned} f(s) = {} & \beta\theta_1(\theta_1')^2 + \frac{\beta}{2}\theta_1^2\theta_1'' + \frac{1}{2}(-\beta\theta_1'' - \theta_1'''')\theta_1^2 + 2(-\beta\theta_1' - \theta_1''')\theta_1\theta_1' \\ & + (-\beta\theta_1 - \theta_1'')(\theta_1')^2 + (-\beta\theta_1 - \theta_1'')\theta_1\theta_1'' \\ & - V''''(D/2)(\theta_1)\left(\frac{-\beta\theta_1' - \theta_1'''}{2V''(D/2)}\right)^2 - V'''(D/2)\theta_1D_2 + \frac{1}{3}V''(D/2)\theta_1^3. \end{aligned} \tag{6.87}$$

Expanding gives

$$f(s) = \beta\theta_1(\theta_1')^2 + \frac{\beta}{2}(\theta_1)^2\theta_1'' - \frac{\beta}{2}\theta_1''(\theta_1)^2 - \frac{1}{2}\theta_1''''(\theta_1)^2 - 2\beta(\theta_1')^2\theta_1 - 2\theta_1'''\theta_1\theta_1' \quad (6.88)$$
$$- \beta\theta_1(\theta_1')^2 - \theta_1''(\theta_1')^2 - \beta(\theta_1)^2\theta_1'' - (\theta_1'')^2\theta_1$$
$$- \frac{V''''(D/2)}{4(V''(D/2))^2}\theta_1(\beta\theta_1' + \theta_1''')^2 - V'''(D/2)\theta_1 D_2 + \frac{1}{3}V''(D/2)\theta_1^3.$$

Inserting into the solvability condition we have

$$\int_0^1 \Big[\beta\theta_1(\theta_1')^2 + \frac{\beta}{2}(\theta_1)^2\theta_1'' - \frac{\beta}{2}\theta_1''(\theta_1)^2 - \frac{1}{2}\theta_1''''(\theta_1)^2 - 2\beta(\theta_1')^2\theta_1 - 2\theta_1'''\theta_1\theta_1' \quad (6.89)$$
$$- \beta\theta_1(\theta_1')^2 - \theta_1''(\theta_1')^2 - \beta(\theta_1)^2\theta_1'' - (\theta_1'')^2\theta_1 - \frac{V''''(D/2)}{4(V''(D/2))^2}\theta_1(\beta\theta_1' + \theta_1''')^2$$
$$- V'''(D/2)\theta_1 D_2 + \frac{1}{3}V''(D/2)\theta_1^3\Big]\bar{v}(x)dx = -H_1(1)\bar{v}'(1) + H_1(0)\bar{v}'(0).$$

Splitting up the integral to separate out the term with D_2 we get

$$\int_0^1 \Big[\beta\theta_1(\theta_1')^2 + \frac{\beta}{2}(\theta_1)^2\theta_1'' - \frac{\beta}{2}\theta_1''(\theta_1)^2 - \frac{1}{2}\theta_1''''(\theta_1)^2 - 2\beta(\theta_1')^2\theta_1 - 2\theta_1'''\theta_1\theta_1' \quad (6.90)$$
$$- \beta\theta_1(\theta_1')^2 - \theta_1''(\theta_1')^2 - \beta(\theta_1)^2\theta_1'' - (\theta_1'')^2\theta_1 - \frac{V''''(D/2)}{4(V''(D/2))^2}\theta_1(\beta\theta_1' + \theta_1''')^2$$
$$+ \frac{1}{3}V''(D/2)\theta_1^3\Big]\bar{v}(x)dx - D_2\int_0^1 V'''(D/2)\theta_1\bar{v}(x)dx = -H_1(1)\bar{v}'(1) + H_1(0)\bar{v}'(0).$$

We define

$$I_1 = \int_0^1 \Big[\beta\theta_1(\theta_1')^2 + \frac{\beta}{2}(\theta_1)^2\theta_1'' - \frac{\beta}{2}\theta_1''(\theta_1)^2 - \frac{1}{2}\theta_1''''(\theta_1)^2 - 2\beta(\theta_1')^2\theta_1 - 2\theta_1'''\theta_1\theta_1' \quad (6.91)$$
$$- \beta\theta_1(\theta_1')^2 - \theta_1''(\theta_1')^2 - \beta(\theta_1)^2\theta_1'' - (\theta_1'')^2\theta_1 - \frac{V''''(D/2)}{4(V''(D/2))^2}\theta_1(\beta\theta_1' + \theta_1''')^2$$
$$+ \frac{1}{3}V''(D/2)\theta_1^3\Big]\bar{v}(x)dx.$$

Solving (6.90) for D_2, we have the following formula,

$$D_2 = \frac{H_1(1)\bar{v}'(1) - H_1(0)\bar{v}'(0) + I_1}{\int_0^1 V'''(D/2)\theta_1\bar{v}(x)dx}. \quad (6.92)$$

The integral here depends on the parameters ω, σ, and on β. In Chapter 7 below, when we do the parametric study, we compute this integral in specific cases to compute a numerical value for D_2. Determining the sign of D_2 will be critical in the bifurcation analysis.

CHAPTER VII

PARAMETRIC STUDY OF D_2

Now using the formula (6.92) we can perform a parametric study of the sign of D_2 for different values of the parameters σ and ω, where σ is the Van der Waals radius and ω is the Van der Waals strength. We use the code in Appendix B to calculate D_2 along the curve of first bifurcation points found earlier. We vary the parameters in order to see points where D_2 will change signs. Recall that the importance of the sign of D_2 is discussed in Section 1.5.

7.1 The Curve of First Bifurcation Points

Before we begin however, it is important to understand more about the curve of first bifurcation points. For a given ω and σ, there is a curve in the βD-plane that represents the location of first bifurcation points (Figure 4.3). More precisely, for a fixed β, as D is increased from a small initial value, there is some smallest D at which the graphene buckles out of its straight configuration. The curve of first bifurcation points is the set of such βD pairs. Physically, we can think of this as the first time the graphene sheet overcomes the Van der Waals of the rigid substrates. When D is relatively small, so that the substrates are close together, the sheet cannot change configuration due to the fixed load β because the rigid substrates apply too strong

transverse compressive force. Once the distance D is increased just enough, the Van der Waals forces will be weak enough to where the sheet buckles for the first time.

We note that the curve of first bifurcation points always has the same basic shape regardless of the value of σ and ω. See Figures (7.1), (7.2) below. This makes physical sense because we always expect the distance D of the first buckling to be slightly less for slightly more force β. This function should always be decreasing because the greater the force applied to the edges of the sheet, the larger the compressive force at which the sheet will buckle, which corresponds to a smaller separation D. Since ω and σ only dictate how the Van der Waals force acts, changing these parameters will result in shifts of the curve of first bifurcation points, but for a specific σ and ω we still expect the separation D to continuously decrease as β is increased.

Looking at Figure 7.1 we can see that all of the curves of first bifurcation points are approximately shifted downward as σ decreases. This makes physical sense because σ is defined as the Van der Waals radius, which we can think of as the distance over which the influence of the Van der Waals force is significant. For larger Van der Waals radius and fixed load β the distance D at which the first buckling occurs for the curves is also greater. Relating this back to the physical setting, we need to pull the substrates further apart as the influence of the Van der Waals is longer in order for the sheet to buckle and overcome the Van der Waals forces. We also note that the Van der Waals is strongly compressive when separations are approximately less than 2σ.

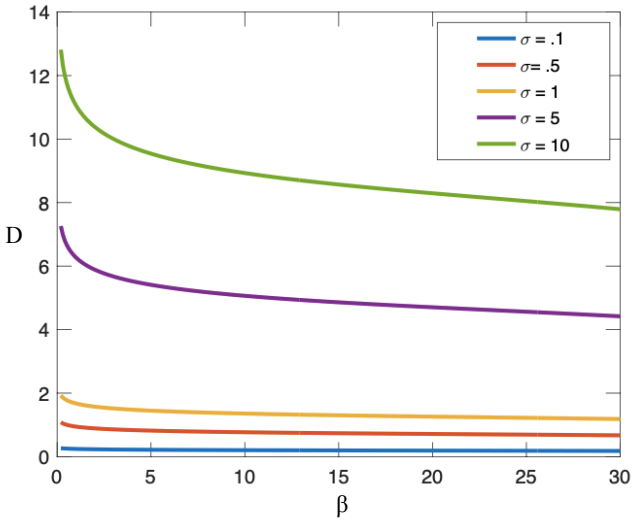

Figure 7.1: Plot of first bifurcation points for fixed $\omega = .01$ and varied σ.

Looking at Figure 7.2 we can see that the curves of first bifurcation points are approximately shifted downward as ω decreases. Thinking of this in a similar way to the case when σ is varied for fixed ω, we see that since ω denotes the Van der Waals strength, we must pull the substrates further apart when the strength of the Van der Waals is greater in order to get the sheet to overcome this force and buckle.

Note that for the left endpoint of the first bifurcation curves in Figure 7.2 all of the curves seem to tend towards the same value at $\beta = 0$ regardless of ω. This can be seen algebraically when computing the curve of first bifurcation points. In Figure 4.2 we discuss that we compute the β-α curve first in Matlab before computing the β-D curves. To convert from α to D, we recall that we defined

$$\alpha = 2V''(D/2). \tag{7.1}$$

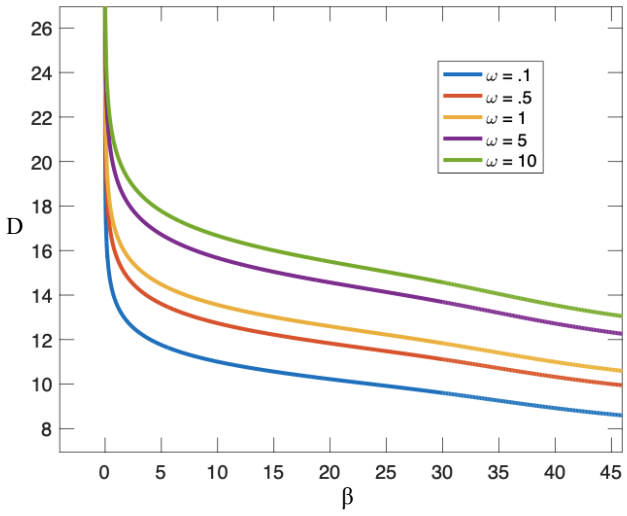

Figure 7.2: Plot of first bifurcation points for fixed $\sigma = 10$ and varied ω.

From Figure 4.2, we see that if $\beta = 0$, then $\alpha = 0$. Then from 7.1 we have

$$0 = V''(D/2) = 2\omega \left(90\sigma^9 \left(\frac{D}{2} \right)^{-11} - 12\sigma^3 \left(\frac{D}{2} \right)^{-5} \right). \tag{7.2}$$

Solving this equation for D yields

$$D = \sqrt[6]{480\sigma^6}. \tag{7.3}$$

So when $\beta = 0$, the curve of first bifurcation points all have the same value since the ccorresponding D value depends on σ but not on ω. Physically we can think that when no load is being applied to the graphene sheet, the strength of the Van der Waals, ω, does not impact the solution.

7.2 The Sign of D_2

Now we will use the curve of first bifurcation points and calculate D_2 using the code in Appendix B. In general, D_2 is a function of ω, σ, D, and β defined using (6.92). However, we can fix parameter values for ω and σ, and then for a given β, we compute the D-value on the curve of first bifurcation points that corresponds to that value of β. We then find D_2 for this combination of ω, σ, β, and D. This procedure allows us to find D_2 as just a function of β along the curve of first bifurcation points corresponding to a given ω and σ.

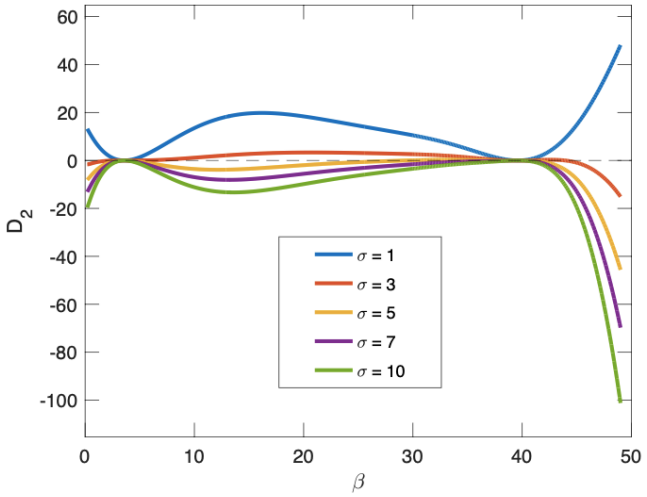

Figure 7.3: Plot of D_2 vs β for fixed $\omega = 1$ and varied σ.

7.2.1 Two Special Values of β

Figure 7.3 shows D_2 as a function of β along the curves of first bifurcation points for $\omega = 1$ and several values of σ. With Figure 7.3 we can note an interesting feature

of these curves as σ is varied. All the curves at $\beta_1^* \approx 3.61$ and $\beta_2^* \approx 39.65$ have a zero independent of σ. To investigate this more closely, we plot the curves on small intervals containing these particular β values.

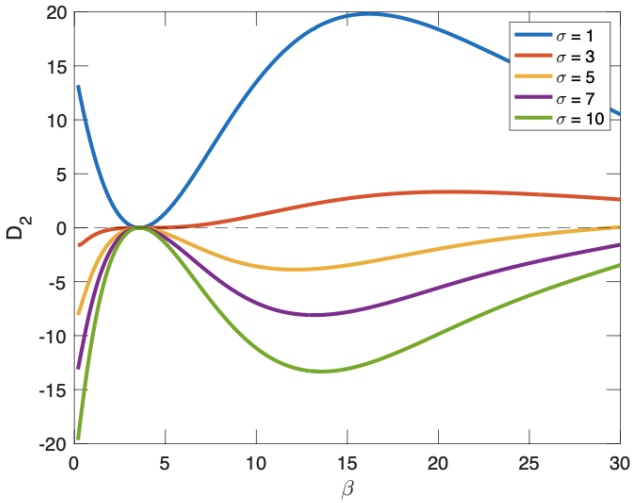

Figure 7.4: Plot of D_2 vs β for fixed $\omega = 1$ and varied σ for $.2 \leq \beta \leq 30$.

For the interval in Figure 7.4 we can see three different behaviors around $\beta_1^* \approx 3.61$. For smaller $\sigma = 1$ we have no sign change and the graph of D_2 stays positive over the interval. For $\sigma = 5$ and higher, we also have no sign change and the graph of D_2 stays negative over the interval. However for $\sigma = 3$, we see a sign change near β_1^* going from negative to positive. Figure 7.5 illustrates more closely which curves do and do not change sign near β_1^*. This sign change is near β_1^* but if one zooms in close enough such as in Figure 7.6, one sees that the sign change occurs somewhere else. For intermediate values of σ in the range $1 \leq \sigma \leq 7$ we see also that

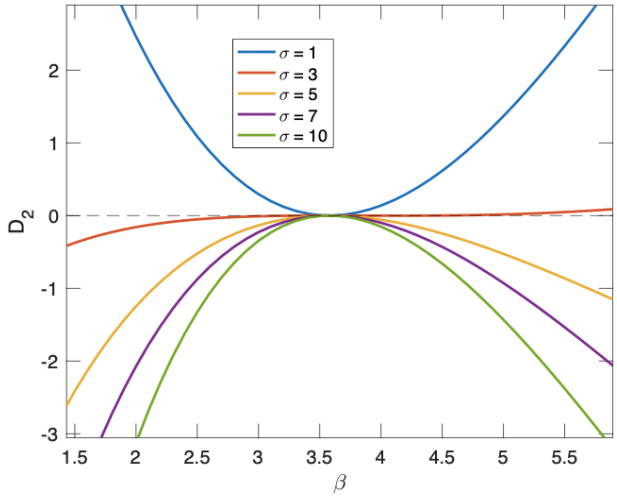

Figure 7.5: Plot of D_2 vs β for fixed $\omega = 1$ and varied σ close to zero value.

we are getting a sign change from negative to positive on this interval of β and the critical value of β that causes this sign change increases as σ increases.

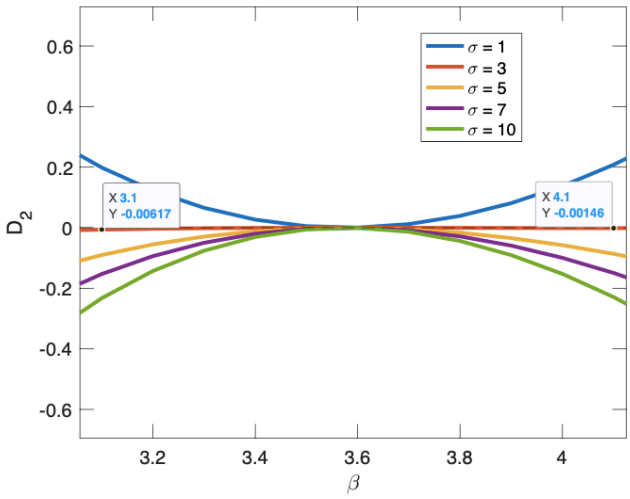

Figure 7.6: Plot of D_2 vs β for fixed $\omega = 1$ and varied σ near β_1^*.

We also note the special value of $\beta_2^* \approx 39.65$ shows a similar behavior as the first zero at $\beta_1^* \approx 3.61$. For a typical ω and σ, if one zooms in close enough about β_2^*, one will see that there is no sign change in D_2 at β_2^*. The formula for D_2 contains terms that depend on ω and σ only through V''. Recall that $A = V''(D/2)$ where V'' also depends on σ and ω. These terms will depend only on β and A. On the curve of first bifurcation points, A is a function of β. Hence on the curve of first bifurcation points these terms depend only on β and these terms have zeros at β_1^* and β_2^*. These terms appear in the formula for D_2 in such a way that when they are zero, D_2 is zero. Therefore D_2 has zeros at β_1^* and β_2^* independent of ω and σ.

7.2.2 D_2 for fixed ω

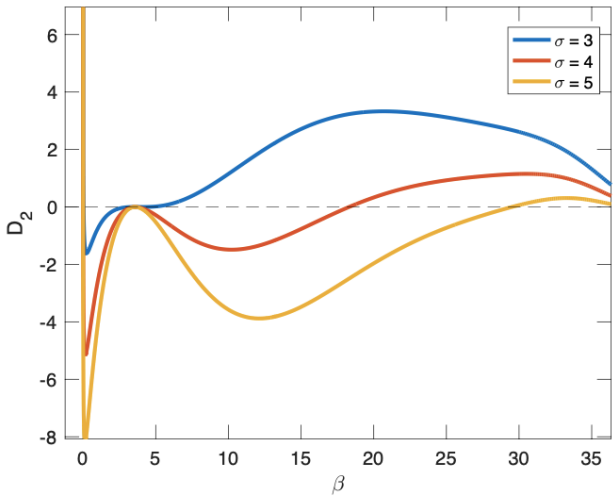

Figure 7.7: Plot of D_2 vs β for fixed $\omega = 1$ and varied σ in the range $3 \leq \sigma \leq 5$

Now we study the sign change in D_2 as the parameter σ is varied for fixed ω.

Here in Figure 7.7 we note that as σ increases, the β value at which the sign of D_2 changes also increases.

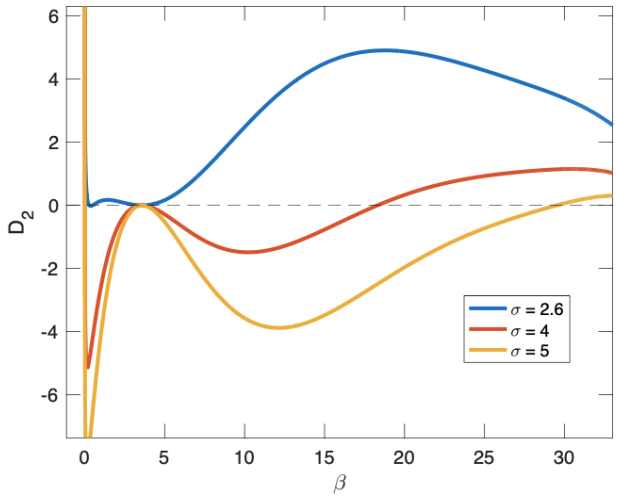

Figure 7.8: Plot of D_2 vs β for fixed $\omega = 1$ and varied σ in the range $2.6 \leq \sigma \leq 5$

For σ less that approximately 2.6, D_2 is positive for all β in the interval for which we have data. This can been seen in Figure 7.8. Then as σ is increased, a small interval on which D_2 is negative is formed. As σ is further increased, the left end point of this interval moves to the left and the right endpoint moves to the right.

We see a similar story for $\omega = .1$ in Figure 7.9 with D_2 being positive over all β with $\sigma \leq 2.6$. We see that for this value of $\omega = .1$ that the interval where the D_2 curve is negative is very small, indicated by the point marked in Figure 7.9.

However, when $\omega = 10$ in Figure 7.10 we see that the D_2 curve for $\sigma = 2.6$ does not develop the little dip that will expand into the interval of negative D_2 curve and the curve is somewhat flat around $\beta = 3$. We also note that D_2 becomes negative

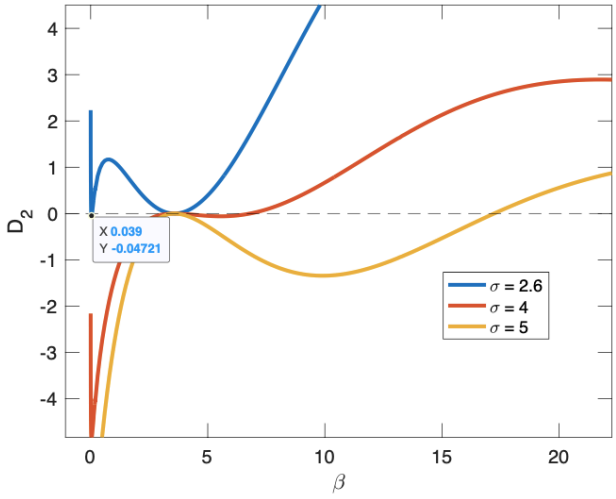

Figure 7.9: Plot of D_2 vs β for fixed $\omega = .1$ and varied σ in the range $2.6 \leq \sigma \leq 5$

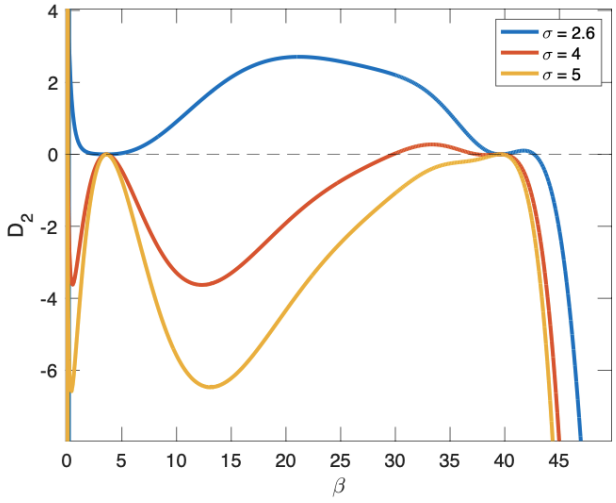

Figure 7.10: Plot of D_2 vs β for fixed $\omega = 10$ and varied σ in the range $2.6 \leq \sigma \leq 5$

when $\beta \approx 42$. This may suggest that for $\omega = .1$ or $\omega = 1$ that the D_2 curves for $\sigma = 2.6$ do actually become negative but just for larger β values outside of the range

of β we are studying.

7.2.3 D_2 for fixed σ

We now look at a particular fixed σ value of $\sigma = 4$. For this value of σ we will denote the first time the D_2-β curve crosses the D_2 axis as $\beta^*(\omega)$ for some value of ω. We then plot these β^* values against their ω values.

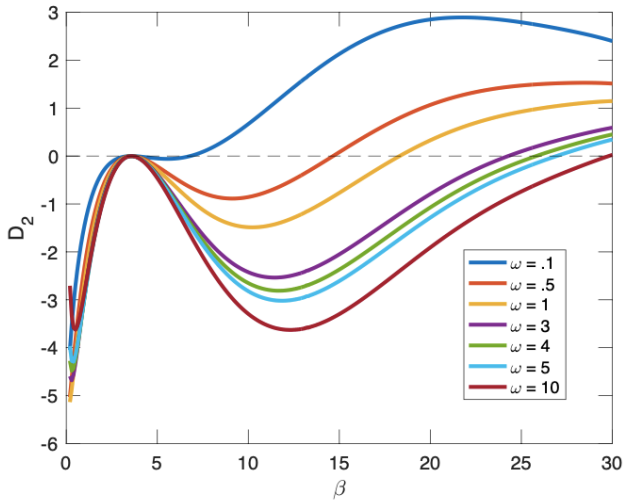

Figure 7.11: Plot of D_2 vs β for fixed $\sigma = 4$ and varied ω.

In Figure 7.11 we see where the values of β^* are being found. In this plot we can also see the increasing trend quite plainly. We then see in Figure 7.12 that the value of β^* increases in an almost logarithmic fashion as ω increases.

Now we continue on to see how the curves of D_2 change when we fix σ and vary ω. For some curves, we have a D_2 value less than zero for the full interval from $.2 \leq \beta \leq 30$ while others are fully positive and intermediate values tend to cross the

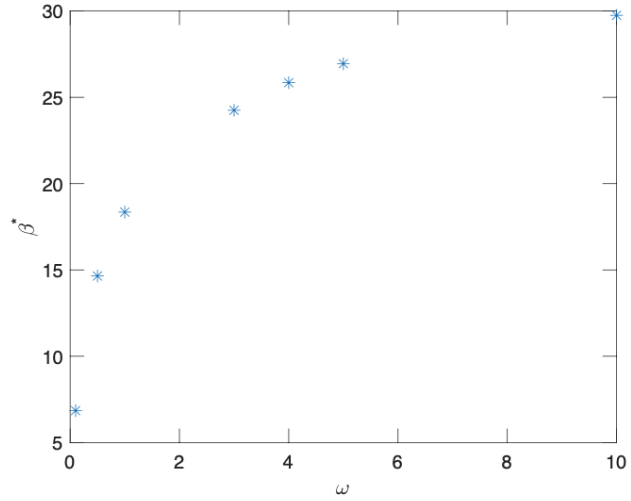

Figure 7.12: Plot of β^* vs ω for fixed $\sigma = 4$.

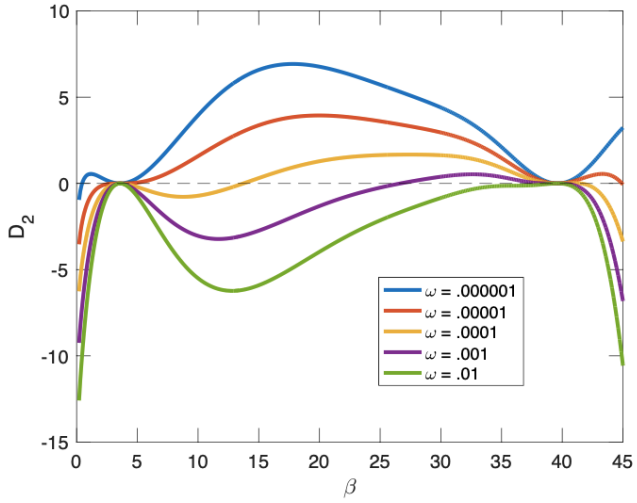

Figure 7.13: Plot of D_2 vs β for fixed $\sigma = 10$ and varied ω.

D_2 axis. We see a similar trend where an increase in ω values causes the curves to become more and more negative and eventually not cross the D_2 axis at all. This is

analogous to what happened in the varied ω case. However we should note that even though the fixed value for Figure 7.13 is an order of magnitude greater than that in Figure 7.3, the values needed to get curves that cross the D_2 axis are much smaller.

CHAPTER VIII

CONCLUSION

We have used the experiment from Barsoum et al. to model and analyze the buckling of a single layer of graphene sandwiched between 2 rigid substrates. Recall that for the model, we have two rigid parallel substrates above and below a single deformable graphene layer. We then apply a fixed load β to each end of the deformable layer and vary the distance D between the rigid substrates. We assume that the graphene layer interacts with each of the substrates by Van der Waals forces. When D is relatively small, so that both the upper and the lower substrates strongly repel the layer, the substrates provide a transverse load that is compressive in the sense that it tries to keep the the layer unbuckled. Loosely speaking, the layer is squeezed between the substrates. The layer also has an intrinsic resistance to bending that tries to keep it unbuckled. On the other hand, the load β on the edges tries to make the layer buckle. If we start with D small and increase the value of D, while keeping β fixed, there should be a critical D at which the layer buckles.

From the parametric study in Chapter 7 we were able to understand the behavior of the sign of D_2. We found that there is some interval of β where D_2 is negative. This interval of β is unique for different σ and ω. When σ is fixed and ω is varied, increasing the value of ω causes this interval where the D_2 curve is negative

to grow wider, with the left endpoint moving towards zero and the right endpoint increasing to larger values of β. Similarly, when σ is varied and ω is fixed, we see the same behavior of the D_2 curves. Additionally, if the values of σ and ω are too small or too large, then we have no change in sign and D_2 is either fully positive or fully negative over the viewing interval. We can infer then that when we have a combination of parameters that contains a sign change, increasing the edge-load β causes large changes in the buckling of the system.

We also found that for the curves that change sign, there is a second sign after a critical value β_2^* where the graphs of D_2 have a zero and do not change sign. These changes in sign of D_2 relate to different types of bifurcations, either subcritical or supercritical. When $D_2 > 0$ then we have supercritical bifurcations where the graphene layer deforms in a controlled and small buckling fashion. When $D_2 < 0$ then we have subcritical bifurcations where the graphene layer deforms suddenly into a far away buckling configuration.

If work were to continue on this project, there are a couple of different areas of interest. For one, it would be interesting to see if extending the β values to infinity cause the D_2 curves to continue oscillating or if they never change sign again. Additionally, more work could be done to understand what exactly happens at the zero values of $\beta_1^* \approx 3.61$ and $\beta_2^* \approx 39.65$ and how we can find these values exactly from the formula for D_2 (6.92). Additionally, it would be interesting to understand where exactly the D_2 curves stop changing signs for fixed σ and varied ω and fixed ω and varied σ. In Chapter 7 we gave a wide range for large integer values of σ and fixed

$\omega = 1$ where the D_2 curves change sign but it could be beneficial to see exactly where these critical σ values are and where they come from. It would also be interesting to create actual plots with the data for figures like Figure 1.6 and Figure 1.5 to see the bifurcation diagrams in reality to get an even better understanding of the subcritical and supercritical bifurcations for this graphene buckling problem.

BIBLIOGRAPHY

[1] Graphene composite innovation day, 2017.

[2] Barsoum, M. W., X. Zhao, S. Shanazarov, A. Romanchuk, S. Koumlis, S. J. Pagano, L. Lamberson, and G. J. Tucker. Ripplocations: A universal deformation mechanism in layered solids. *Phys. Rev. Materials*, 3:013602, 2019.

[3] Kumar, A., K. Sharma and A. R. Dixit. A review of the mechanical and thermal properties of graphene and its hybrid polymer nanocomposites for structural applications. *Journal of Materials Science*, 54:5992–6026, 2019.

[4] Shimada, T., K. Huang, L. V. Lich, N. Ozaki, B. Jang, and T. Kitamura. Beyond conventional nonlinear fracture mechanics in graphene nanoribbons. *Nanoscale*, 12:18363, 2020.

[5] Behfar, K., P. Seifi, R. Naghdabadi and J. Ghanbari. An analytical approach to determination of bending modulus of a multi-layered graphene sheet. *Thin Solid Films*, 496:475–480, 2006.

[6] Akinwande, D., C. J. Brennan, J. S. Bunch, P. Egberts, J. R. Felts, H. Gao, R. Huang, J. S. Kim, T. Li, Y. Li, K. M. Liechti, N. Lu, H. S. Park, E. J. Reed, P. Wang, B. I. Yakobson, T. Zhang, Y. W. Zhang, Y. Zhou, and Y. Zhu. A review on mechanics and mechanical properties of 2d materials—graphene and beyond. *Extreme Mechanics Letters*, 13:42–77, 2017.

[7] Cao, Q., X. Geng, H. Wang, P. Wang, A. Liu, Y. Lan, and Q. Peng. A review of current development of graphene mechanics. *Crystals*, 8(9), 2018.

[8] Pop, E., V. Varshney and A. K. Roy. Thermal properties of graphene: Fundamentals and applications. *MRS Bulletin*, 37:1273–1281, 2012.

[9] Barsoum, M.W. and G.J. Tucker. Deformation of layered solids: Ripplocations not basal dislocations. *Scripta Materialia*, 139:166–172, 2017.

[10] Gruber, J., A.C. Lang, J. Griggs, M.L. Taheri, G.J. Tucker, and M.W. Barsoum. Evidence for bulk ripplocations in layered solids. *Scientific Reports*, 6, 2016.

[11] Kushima, A., X. Qian, P. Zhao, S. Zhang, and J. Li. Ripplocations in van der waals layers. *Nano Letters*, 15:1302–1308, 2015.

[12] E.A. Coddington and N. Levinson. *Theory of Ordinary Differential Equations*. McGraw-Hill, NewYork, 1955.

APPENDICES

APPENDIX A

MATLAB CODE BIFURCATION POINTS

```
1
2
3  K=30;
4  bs = .2:.1:K;
5
6  sol = zeros(length(bs),1);
7
8  for k = 1:length(bs)
9        b0=bs(k);
10       if k == 1
11           x = linspace(2,50,1000);
12       else
13           x = linspace(sol(k-1),600,100000);
14       end
15 val = zeros(length(x),1);
16
17 for i = 1:length(x)
```

```
18      val(i) = abs(Determinant(x(i),b0));
19  end
20
21  TF = islocalmin(val);
22  if abs(x(find(TF,1,'first'))-((b0^2)/4))<.01
23      TF(find(TF,1,'first'))=0;
24      I = find(TF, 1, 'first');
25  else
26      I = find(TF, 1, 'first');
27  end
28  sol(k)=x(I);
29
30  end
31  plot(bs,sol)
32  title('a vs b')
33
34  sig = 1;
35  w = .001;
36  sol2 = zeros(length(sol),1);
37
38  for k = 1:length(sol)
```

```
39
40      p = [sol(k)/(2*w),0,0,0,0,384*(sig)^3,0,0,0,0,0,-184320*(
            sig)^9];
41      r = roots(p);
42      TF2 = (imag(r)==0);
43      I = find(TF2, 1, 'first');
44      sol2(k)=r(I);
45  end
46  plot(bs,sol2)
47
48
49  function [f,Q] = Determinant(a,b)
50
51  discrim = sqrt(b^2-(4*a));
52  m1 = sqrt((-b+discrim)/2);
53  m2 = sqrt((-b-discrim)/2);
54  m3 = -sqrt((-b+discrim)/2);
55  m4 = -sqrt((-b-discrim)/2);
56
57  Q = [m1,m2,m3,m4;m1*exp(m1),m2*exp(m2),m3*exp(m3),m4*exp(m4);
58       (b+m1^2),(b+m2^2),(b+m3^2),(b+m4^2);
```

```
59      (b+m1^2)*exp(m1),(b+m2^2)*exp(m2),(b+m3^2)*exp(m3),(b+m4
            ^2)*exp(m4)];
60
61  f = det(Q);
62  end
```

APPENDIX B

MATLAB CODE PLOTTING D_2

```
1
2
3  numPoints = length(sol);
4  sigma = sig;
5  d2s = zeros(numPoints,1);
6  tops = zeros(numPoints,1);
7  botts = zeros(numPoints,1);
8
9  a = sol;
10 b = bs';
11 d = sol2;
12
13 discrim = sqrt(b.^2-(4.*a));
14
15 m_minus = sqrt((-b-discrim)./2);
16 m_plus = sqrt((-b+discrim)./2);
17 m1 = -m_plus;
```

```
18 m2 = m_plus;
19 m3 = -m_minus;
20 m4 = m_minus;
21 e1 = exp(-m_plus);
22 e2 = exp(m_plus);
23 e3 = exp(-m_minus);
24 e4 = exp(m_minus);
25
26 handc4 = ones(numPoints,1);
27 handSigmaPart2 = ((b+m1.^2).*m2.*e2./(m1.*e1))-b-m2.^2;
28 handSigmaPart3 = -((b+m1.^2).*m3.*e3./(m1.*e1))+b+m3.^2;
29 handSigmaPart4 = -((b+m1.^2).*m4.*e4./(m1.*e1))+b+m4.^2;
30 handSigma3 = (handSigmaPart2.*(m3.*(e3-e1))./(m2.*(e2-e1)))+
       handSigmaPart3;
31 handSigma4 = (handSigmaPart2.*(m4.*(e4-e1))./(m2.*(e2-e1)))+
       handSigmaPart4;
32 handc3 = -handSigma4./handSigma3;
33 handc2 = ((-m3.*(e3-e1).*handc3)-(m4.*(e4-e1)))./(m2.*(e2-e1)
       );
34 handc1 = (-m2.*handc2 - m3.*handc3 - m4)./m1;
35 smallSigmaPart2 = -handSigmaPart2;
```

```
36
37 smallSigma3 = ((-(b+m2.^2).*(e2-e1).*handSigmaPart3)./
       smallSigmaPart2)+(b+m3.^2).*(e3-e1);
38 smallSigma4 = ((-(b+m2.^2).*(e2-e1).*handSigmaPart4)./
       smallSigmaPart2)+(b+m4.^2).*(e4-e1);
39
40 big3 = smallSigma3./handSigma3;
41 big4 = smallSigma4./handSigma4;
42
43 c1 = handc1;
44 c2 = handc2;
45 c3 = handc3;
46 c4 = handc4;
47
48 rrefgamma2 = (e2-e1).*m2.^3;
49 rrefgamma3 = (e3-e1).*m3.^3;
50 rrefgamma4 = (e4-e1).*m4.^3;
51 rrefbeta2 = m2.^3 -(e2./e1).*m1.^3;
52 rrefbeta3 = m3.^3 -(e3./e1).*m1.^3;
53 rrefbeta4 = m4.^3 -(e4./e1).*m1.^3;
54 rrefsmallSig2 = (e2-e1);
```

```
55 rrefsmallSig3 = (e3-e1);
56 rrefsmallSig4 = (e4-e1);
57 rrefalpha3 = rrefbeta3 - (rrefbeta2./rrefsmallSig2).*
       rrefsmallSig3;
58 rrefalpha4 = rrefbeta4 - (rrefbeta2./rrefsmallSig2).*
       rrefsmallSig4;
59
60 rrefc4 = ones(numPoints,1);
61 rrefc3 = -rrefalpha4.*rrefc4./rrefalpha3;
62 rrefc2 = (-rrefsmallSig4.*rrefc4 -rrefsmallSig3.*rrefc3)./
       rrefsmallSig2;
63 rrefc1 = -rrefc2 -rrefc3 -rrefc4;
64
65
66 for i = 1:numPoints
67 h_1 = @(x) real(rrefc3(i)*(-m_minus(i))*exp(-m_minus(i)*x)+
       rrefc4(i)*(m_minus(i))*exp(m_minus(i)*x)+rrefc2(i)*(m_plus
       (i))*exp(m_plus(i)*x)+rrefc1(i)*(-m_plus(i))*exp(-m_plus(i
       )*x));
68
69 H1 = @(x) (b(i)/6)*(real(c3(i)*exp(-m_minus(i)*x)+c4(i)*exp(
```

```
    m_minus(i)*x)+c2(i)*exp(m_plus(i)*x)+c1(i)*exp(-m_plus(i)*
    x)))^3 - .5*(b(i)*real(c3(i)*exp(-m_minus(i)*x)+c4(i)*exp(
    m_minus(i)*x)+c2(i)*exp(m_plus(i)*x)+c1(i)*exp(-m_plus(i)*
    x)) ...
70      + real(c3(i)*((-m_minus(i))^2)*exp(-m_minus(i)*x)+c4(i)
          *((m_minus(i))^2)*exp(m_minus(i)*x)+c2(i)*(m_plus(i)
          ^2)*exp(m_plus(i)*x)+c1(i)*((-m_plus(i))^2)*exp(-
          m_plus(i)*x)) ...
71      )*(real(c3(i)*exp(-m_minus(i)*x)+c4(i)*exp(m_minus(i)*x)
          +c2(i)*exp(m_plus(i)*x)+c1(i)*exp(-m_plus(i)*x)))^2;
72
73  bigIntinside1 = @(x) (-2.*b(i).*real(c3(i).*exp(-m_minus(i).*
    x)+c4(i).*exp(m_minus(i).*x)+c2(i).*exp(m_plus(i).*x)+c1(i
    ).*exp(-m_plus(i).*x)).*(real(c3(i).*(-m_minus(i)).*exp(-
    m_minus(i).*x)+c4(i).*(m_minus(i)).*exp(m_minus(i).*x)+c2(
    i).*(m_plus(i)).*exp(m_plus(i).*x)+c1(i).*(-m_plus(i)).*
    exp(-m_plus(i).*x)) ...
74    ).^2 - .5.*real(c3(i).*((-m_minus(i)).^4).*exp(-m_minus(
        i).*x)+c4(i).*((m_minus(i)).^4).*exp(m_minus(i).*x)+c2
        (i).*(m_plus(i).^4).*exp(m_plus(i).*x)+c1(i).*((-
        m_plus(i)).^4).*exp(-m_plus(i).*x)).*(real(c3(i).*exp
```

```
        (-m_minus(i).*x)+c4(i).*exp(m_minus(i).*x)+c2(i).*exp(
        m_plus(i).*x)+c1(i).*exp(-m_plus(i).*x)) ...
75      ).^2 - 2.*real(c3(i).*exp(-m_minus(i).*x)+c4(i).*exp(
        m_minus(i).*x)+c2(i).*exp(m_plus(i).*x)+c1(i).*exp(-
        m_plus(i).*x)).*real(c3(i).*(-m_minus(i)).*exp(-
        m_minus(i).*x)+c4(i).*(m_minus(i)).*exp(m_minus(i).*x)
        +c2(i).*(m_plus(i)).*exp(m_plus(i).*x)+c1(i).*(-m_plus
        (i)).*exp(-m_plus(i).*x)) ...
76      .*real(c3(i).*((-m_minus(i)).^3).*exp(-m_minus(i).*x)+c4(
        i).*((m_minus(i)).^3).*exp(m_minus(i).*x)+c2(i).*(
        m_plus(i).^3).*exp(m_plus(i).*x)+c1(i).*((-m_plus(i))
        .^3).*exp(-m_plus(i).*x))).*real(rrefc3(i).*exp(-
        m_minus(i).*x)+rrefc4(i).*exp(m_minus(i).*x)+rrefc2(i)
          ...
77      .*exp(m_plus(i).*x)+rrefc1(i).*exp(-m_plus(i).*x));
78
79  bigIntinside2 = @(x) (-real(c3(i).*((-m_minus(i)).^2).*exp(-
      m_minus(i).*x)+c4(i).*((m_minus(i)).^2).*exp(m_minus(i).*x
      )+c2(i).*(m_plus(i).^2).*exp(m_plus(i).*x)+c1(i).*((-
      m_plus(i)).^2).*exp(-m_plus(i).*x)) ...
80      .*(real(c3(i).*(-m_minus(i)).*exp(-m_minus(i).*x)+c4(i)
```

```
    .*(m_minus(i)).*exp(m_minus(i).*x)+c2(i).*(m_plus(i))
    .*exp(m_plus(i).*x)+c1(i).*(-m_plus(i)).*exp(-m_plus(i
    ).*x)) ...
81  ).^2 - real(c3(i).*exp(-m_minus(i).*x)+c4(i).*exp(m_minus
    (i).*x)+c2(i).*exp(m_plus(i).*x)+c1(i).*exp(-m_plus(i)
    .*x)) ...
82  .*(real(c3(i).*((-m_minus(i)).^2).*exp(-m_minus(i).*x)+c4
    (i).*((m_minus(i)).^2).*exp(m_minus(i).*x)+c2(i).*(
    m_plus(i).^2).*exp(m_plus(i).*x)+c1(i).*((-m_plus(i))
    .^2).*exp(-m_plus(i).*x))).^2 - b(i).*real(c3(i).*((-
    m_minus(i)).^2).*exp(-m_minus(i).*x)+c4(i).*((m_minus(
    i)).^2).*exp(m_minus(i).*x)+ ...
83  c2(i).*(m_plus(i).^2).*exp(m_plus(i).*x)+c1(i).*((-m_plus
    (i)).^2).*exp(-m_plus(i).*x)) ...
84  .*(real(c3(i).*exp(-m_minus(i).*x)+c4(i).*exp(m_minus(i)
    .*x)+c2(i).*exp(m_plus(i).*x)+c1(i).*exp(-m_plus(i).*x
    )) ...
85  ).^2).*real(rrefc3(i).*exp(-m_minus(i).*x)+rrefc4(i) ...
86  .*exp(m_minus(i).*x)+rrefc2(i).*exp(m_plus(i).*x)+rrefc1(
    i).*exp(-m_plus(i).*x));
87
```

```
88  bigIntinside3 = @(x) (-((w.*((-360.*sigma.^3).*(d(i)/2)
        .^(-7) + (11880.*sigma.^9).*(d(i)/2).^(-13))).*(4.*((w
        .*((-12.*sigma.^3).*(d(i)/2).^(-5) + (90.*sigma.^9).*(d(i
        )/2).^(-11))).^2))).*real(c3(i).*exp(-m_minus(i).*x)+c4(i
        ).*exp(m_minus(i).*x)+c2(i).*exp(m_plus(i).*x)+c1(i).*exp
        (-m_plus(i).*x)) ...
89          .*(real(c3(i).*((-m_minus(i)).^3).*exp(-m_minus(i).*x)+c4
                (i).*((m_minus(i)).^3).*exp(m_minus(i).*x)+c2(i).*(
                m_plus(i).^3).*exp(m_plus(i).*x)+c1(i).*((-m_plus(i))
                .^3).*exp(-m_plus(i).*x)) ...
90          + b(i).*real(c3(i).*(-m_minus(i)).*exp(-m_minus(i).*x)+c4
                (i).*(m_minus(i)).*exp(m_minus(i).*x)+c2(i).*(m_plus(i
                )).*exp(m_plus(i).*x)+c1(i).*(-m_plus(i)).*exp(-m_plus
                (i).*x)) ...
91          ).^2 + ...
92          (1./3).*(w.*((-12.*sigma.^3).*(d(i)/2).^(-5) + (90.*sigma
                .^9).*(d(i)/2).^(-11))).*(real(c3(i).*exp(-m_minus(i)
                .*x)+c4(i).*exp(m_minus(i).*x)+c2(i).*exp(m_plus(i).*x
                )+c1(i).*exp(-m_plus(i).*x)) ...
93          ).^3).*real(rrefc3(i).*exp(-m_minus(i).*x)+rrefc4(i) ...
```

```
94        .*exp(m_minus(i).*x)+rrefc2(i).*exp(m_plus(i).*x)+rrefc1(
              i).*exp(-m_plus(i).*x));
95
96  bigInt1 = integral(bigIntinside1,0,1);
97  bigInt2 = integral(bigIntinside2,0,1);
98  bigInt3 = integral(bigIntinside3,0,1);
99  integrand2 = @(x) (w.*((60.*sigma.^3).*(d(i)/2).^(-6) -
        (990.*sigma.^9).*(d(i)/2).^(-12))).*real(c3(i).*exp(-
        m_minus(i).*x)+c4(i).*exp(m_minus(i).*x)+c2(i).*exp(m_plus
        (i).*x)+c1(i).*exp(-m_plus(i).*x)).*real(rrefc3(i).*exp(-
        m_minus(i).*x)+rrefc4(i).*exp(m_minus(i).*x)+rrefc2(i).*
        exp(m_plus(i).*x)+rrefc1(i).*exp(-m_plus(i).*x));
100 bottomInt  = integral(integrand2,0,1);
101
102 H1one = H1(1);
103 h_1one = h_1(1);
104
105 H1zero = H1(0);
106 h_1zero = h_1(0);
107
```

```
108 d2s(i) = (bigInt1 + bigInt2 + bigInt3 - H1zero*h_1zero +
        H1one*h_1one)/bottomInt;
109
110 end
111 plot(b,d2s);
```